

PREPARED FOR SUBMISSION TO JHEP

QCD axion from chiral gauge theories

Ryosuke Sato,^a and Shonosuke Takeshita^b

^a *Department of Physics, The University of Osaka, Toyonaka, Osaka 560-0043, Japan*

^b *Physics Program, Graduate School of Advanced Science and Engineering, Hiroshima University, Higashi-Hiroshima 739-8526, Japan*

E-mail: rsato@het.phys.sci.osaka-u.ac.jp, shonosuke@hiroshima-u.ac.jp

ABSTRACT: We present models of axion based on supersymmetric chiral gauge theories. In these models, the PQ symmetry is spontaneously broken by the non-perturbative dynamics of chiral gauge theory. Thanks to supersymmetry, IR dynamics of the models are calculable. We also present an example of a QCD axion model that is compatible with SU(5) grand unification. We find that the PQ breaking scale should be higher than $\sim 10^{13}$ GeV for the successful GUT unification. In addition, the PQ breaking scale should be higher than the GUT scale to avoid a Landau pole of gauge coupling below the Planck scale.

Contents

1	Introduction	1
2	Axion from SUSY chiral gauge theories	2
2.1	Axion from SUSY Georgi-Glashow type model	2
2.2	Axion from SUSY Bars-Yankielowicz type model	7
2.3	Generalization of axion models	10
3	GUT-motivated QCD axion model	10
3.1	Symmetry breaking scale and VEVs	11
3.2	Numerical analysis of coupling unification	13
3.2.1	The case of $M_{\text{PQ}} > M_{\text{GUT}}$	14
3.2.2	The case of $M_{\text{PQ}} < M_{\text{GUT}}$	14
3.3	Proton decay	17
3.4	Small instanton	21
3.5	Cosmology	21
4	Conclusions and discussions	22
A	Dynamical superpotential in SUSY Georgi-Glashow type model	23
B	The GUT breaking VEV σ	25
B.1	The case of $M_{\text{PQ}} > M_{\text{GUT}}$	27
B.2	The case of $M_{\text{PQ}} < M_{\text{GUT}}$	29
C	RGEs	31
C.1	Input parameters	31
C.2	MSSM	31
C.3	Minimal SU(5) GUT	32
C.4	MSSM with Georgi-Glashow type model	33
C.5	Minimal SU(5) GUT with Georgi-Glashow type model	33
D	RGEs for proton decay	34

1 Introduction

The strong CP problem [1, 2] is one of the most mysterious puzzles in the Standard Model (SM). The effective θ -angle in the QCD sector is severely constrained as $|\bar{\theta}| \lesssim 10^{-10}$ from the null observation of the neutron electric dipole moment (EDM) [3], though $\mathcal{O}(1)$ CP phase has been observed in the Cabibbo-Kobayashi-Maskawa (CKM) matrix. This would

indicate some unknown mechanism to realize the hierarchy $|\delta_{\text{CKM}}| \gg |\bar{\theta}|$ which is incorporated in physics beyond the standard model. The QCD axion [4–7] is one of the most interesting proposals to solve the strong CP problem. It is a pseudo Nambu-Goldstone (NG) boson associated with spontaneous breaking of global $U(1)_{\text{PQ}}$ symmetry which is anomalous under QCD interaction. Since the QCD axion couples to $SU(3)_c$ gauge field via a coupling $(a/32\pi^2 f_a) G_{\mu\nu} \tilde{G}^{\mu\nu}$, the θ -angle is “promoted to a dynamical scalar field”. Then the θ -angle is absorbed by the axion at its potential minimum [8] and the predicted size of the neutron EDM becomes much smaller than the current experimental upperbound [9].

An interesting scenario for the QCD axion would be spontaneous $U(1)_{\text{PQ}}$ breaking induced by strong dynamics of a new gauge interaction [10, 11]. In this case, the order parameter of PQ symmetry breaking is a composite operator. Refs. [12–22] utilize this property to solve the axion quality problem. Most models utilize strong dynamics of QCD-like gauge theories. On the other hand, discussion of the QCD axion based on strong dynamics of chiral gauge theories is quite limited [18, 21] because of the difficulty of the analysis, as chiral gauge theories generally lack analytical tools for studying their non-perturbative dynamics. Recently, Refs. [23, 24] have analyzed the strong dynamics of chiral gauge theories in supersymmetric (SUSY) models with small SUSY breaking [25–32]. Thanks to SUSY, non-perturbative dynamics of chiral gauge theory can be solved in analytic expressions.

In this paper, we apply the analysis in [23, 24] to chiral gauge theories, and show some explicit examples of the QCD axion from chiral gauge theories. This paper is organized as follows. In section 2, we show explicit examples of models. In section 3, we show an example of model of the QCD axion which is compatible with $SU(5)$ grand unification, and discuss its phenomenology and cosmology. Section 4 is devoted to conclusions and discussions. In appendix A, we discuss a dynamical superpotential in $SU(2N)$ chiral gauge theory. In appendix B, we show a detail of calculation of GUT breaking VEV. In appendix C, we list the input parameters and RGEs for coupling constants. In appendix D, we show the RGEs for proton decay operators.

2 Axion from SUSY chiral gauge theories

In this section, we present two simple toy models of chiral gauge theories that include an axion. This axion couples to the $SU(N)$ gauge field through the following interaction:

$$\mathcal{L} = \frac{a}{f_a} \frac{1}{32\pi^2} G_{\mu\nu} \tilde{G}^{\mu\nu}. \quad (2.1)$$

Similar to the analysis presented in Refs. [23, 24], where non-perturbative dynamics of chiral gauge theories were solved using supersymmetry, we utilize SUSY chiral gauge theories with small soft SUSY breaking.

2.1 Axion from SUSY Georgi-Glashow type model

We introduce $SU(2N+4)_1 \times SU(N)_2$ gauge symmetry and chiral multiplets \bar{F}_q ($\bar{\square}, \square$), $\bar{F}_{\bar{q}}$ ($\bar{\square}, \bar{\square}$), and A ($\square, \mathbf{1}$). We assume that the dynamical scale of $SU(N)_2$ gauge symmetry is

	$SU(2N+4)_1$	$SU(N)_2$	$U(1)_{PQ}$	$U(1)_q$	$U(1)_R$	$SU(2N)_{\bar{F}}$
\bar{F}_q	\square	\square	$N+1$	1	0	\square
$\bar{F}_{\bar{q}}$	$\bar{\square}$	$\bar{\square}$	$N+1$	-1	0	
A	\square	$\mathbf{1}$	$-N$	0	$-3/(N+1)$	$\mathbf{1}$

Table 1. Matter content of SUSY Georgi-Glashow model.

much below than that of $SU(2N+4)_1$ gauge symmetry, i.e., $\Lambda_N \ll \Lambda_{2N+4}$. We assume the tree level superpotential W_{tree} to be zero. In this setup, we can find $U(1)_{PQ} \times U(1)_q \times U(1)_R$ global symmetries, which are free from $SU(2N+4)_1$ anomaly. The matter content and the charge assignment under the global symmetries are summarized in Tab. 1. Note that $SU(2N)_{\bar{F}}$ global symmetry arises in the limit of $\Lambda_N \rightarrow 0$ and this $SU(2N)_{\bar{F}}$ global symmetry is equivalent to that of [23]. $SU(N)_2 \times U(1)_q$ can be understood as a subgroup of $SU(2N)_{\bar{F}}$.

Let us discuss the symmetry breaking pattern in the D -flat direction. We write A as $(2N+4) \times (2N+4)$ matrix and \bar{F}_q and $\bar{F}_{\bar{q}}$ as $N \times (2N+4)$ matrix. $SU(2N+4)_1 \times SU(N)_2$ gauge transformation for A , \bar{F}_q , and $\bar{F}_{\bar{q}}$ is given as

$$A \rightarrow UAU^T, \quad \bar{F}_q \rightarrow U^* \bar{F}_q V^T, \quad \bar{F}_{\bar{q}} \rightarrow U^* \bar{F}_{\bar{q}} V^\dagger, \quad (2.2)$$

where $U \in SU(2N+4)_1$ and $V \in SU(N)_2$. D -flat condition is

$$2A^\dagger A - \bar{F}_q \bar{F}_q^\dagger - \bar{F}_{\bar{q}} \bar{F}_{\bar{q}}^\dagger \propto I_{2N}, \quad \bar{F}_q^\dagger \bar{F}_q - \bar{F}_{\bar{q}}^T \bar{F}_{\bar{q}}^* \propto I_N. \quad (2.3)$$

As a solution, we obtain

$$A = \begin{pmatrix} 0_{N \times N} & -icI_N \\ icI_N & 0_{N \times N} \\ & & 0_{2 \times 2} & -ic'I_2 \\ & & ic'I_2 & 0_{2 \times 2} \end{pmatrix}, \quad \bar{F}_q = \phi \begin{pmatrix} I_N \\ 0_{N \times N} \\ 0_{N \times 4} \end{pmatrix}, \quad \bar{F}_{\bar{q}} = \phi \begin{pmatrix} 0_{N \times N} \\ I_N \\ 0_{N \times 4} \end{pmatrix}, \quad (2.4)$$

where c , c' , and ϕ are constants that satisfy $|c|^2 = |\phi|^2 + |c'|^2$. Let us identify the unbroken gauge symmetry in this direction. The VEVs given in eq. (2.4) are invariant under a gauge transformation eq. (2.2) with

$$U = \begin{pmatrix} \tilde{V}_{SU(N)} & & \\ & \tilde{V}_{SU(N)}^* & \\ & & I_4 \end{pmatrix}, \quad V = \tilde{V}_{SU(N)}, \quad (2.5)$$

and

$$U = \begin{pmatrix} I_{2N} & \\ & \tilde{U}_{Sp(4)} \end{pmatrix}, \quad V = I_N. \quad (2.6)$$

Note that $\tilde{V}_{SU(N)} \in SU(N)_d$ and $\tilde{U}_{Sp(4)} \in Sp(4)_1$. $SU(2N+4)_1$ gauge group contains $SU(N)_1 \times Sp(4)_1$ as a subgroup. The gauge transformation eq. (2.5) shows $SU(N)_d$ which

is a diagonal subgroup of $SU(N)_1 \times SU(N)_2$ is unbroken. Also, the gauge transformation eq. (2.6) shows $Sp(4)_1 \in SU(2N+4)_1$ is unbroken. The $SU(N)_d$ gauge coupling is determined by the following matching condition at tree level:

$$\frac{1}{\alpha_{SU(N)_d}} = \frac{1}{\alpha_{SU(2N+4)_1}} + \frac{1}{\alpha_{SU(N)_2}}. \quad (2.7)$$

The VEVs eq. (2.4) spontaneously break both $U(1)_{PQ}$ and $U(1)_R$ symmetry. On the other hand, we can find the VEVs are invariant under the following combination of $U(1)_q$ transformation,

$$\bar{F}_q \rightarrow e^{i\alpha} \bar{F}_q, \quad \bar{F}_{\bar{q}} \rightarrow e^{-i\alpha} \bar{F}_{\bar{q}}, \quad (2.8)$$

and $U(1)_1 (\subset SU(2N+4)_1)$ gauge transformation eq. (2.2) with

$$U = \begin{pmatrix} e^{i\alpha} I_N & & \\ & e^{-i\alpha} I_N & \\ & & I_4 \end{pmatrix}, \quad V = I_N. \quad (2.9)$$

Thus, the VEVs eq. (2.4) are invariant under the $U(1)_d$ transformation which is a diagonal subgroup of $U(1)_q \times U(1)_1$. To summarize, symmetry breaking pattern by the VEVs eq. (2.4) is

$$[SU(2N+4)_1 \times SU(N)_2] \times U(1)_{PQ} \times U(1)_q \times U(1)_R \rightarrow [Sp(4)_1 \times SU(N)_d] \times U(1)_d. \quad (2.10)$$

Here, the square brackets $[\dots]$ indicate the gauge symmetries, while the terms outside the brackets represent the global symmetries.

Let us discuss how this D -flat direction is stabilized by SUSY breaking. In the D -flat direction, $Sp(4)_1$ gauge symmetry is unbroken. The dynamical scale of $Sp(4)_1$ is given as

$$\Lambda_{Sp(4)} = 2^{-(N+2)/9} \left(\frac{\Lambda_{2N+4}^{4N+11}}{(\text{Pf} A \bar{F} \bar{F})(\text{Pf} A)} \right)^{1/9}, \quad (2.11)$$

and its gaugino condensation induces the dynamical superpotential as [33, 34]

$$W = 3 \cdot 2^{-(1+N)/3} \left(\frac{\Lambda_{2N+4}^{4N+11}}{(\text{Pf} A \bar{F} \bar{F})(\text{Pf} A)} \right)^{1/3}. \quad (2.12)$$

See appendix A for details. This leads to a runaway scalar potential for \bar{F} and A . Let us introduce soft SUSY breaking masses to stabilize the vacuum:

$$V_{\text{soft}} = m^2 |\bar{F}_q|^2 + m^2 |\bar{F}_{\bar{q}}|^2 + m^2 |A|^2. \quad (2.13)$$

Here we assume the universal soft SUSY breaking scalar masses. At the global minimum of the scalar potential $V = \sum_{X=A, \bar{F}_q, \bar{F}_{\bar{q}}} |\partial W / \partial X|^2 + V_{\text{soft}}$, ϕ and c in eq. (2.4) are given as

$$\phi = x_N \Lambda_{2N+4} \left(\frac{\Lambda_{2N+4}}{m} \right)^{3/(4N+8)}, \quad c = y_N \Lambda_{2N+4} \left(\frac{\Lambda_{2N+4}}{m} \right)^{3/(4N+8)}, \quad (2.14)$$

N	x_N	y_N	z_N	w_N
1	0.993	1.23	0.813	0.213
3	0.951	1.15	0.706	0.233
5	0.923	1.10	0.646	0.213
10	0.887	1.03	0.566	0.172
30	0.851	0.941	0.459	0.107

Table 2. x_N and y_N in eq. (2.14), z_N in eq. (2.15), and w_n in eq. (2.28) for $N = 1, 3, 5, 10, 30$.

where x_N and y_N are $\mathcal{O}(1)$ coefficients determined by N . For its numerical value, see Tab. 2. For $m \ll \Lambda_{2N+4}$, these VEVs are larger than Λ_{2N+4} and it justifies our weakly coupled analysis. Then, the dynamical scale of $\text{Sp}(4)$ is

$$\Lambda_{\text{Sp}(4)} = z_N \Lambda_{2N+4} \left(\frac{\Lambda_{2N+4}}{m} \right)^{-(2N+1)/(6N+12)}. \quad (2.15)$$

z_N is $\mathcal{O}(1)$ coefficient determined by N . For its numerical value, see Tab. 2. In addition to scalar soft masses, we can also add SUSY breaking which also violates R symmetry. For example, anomaly-mediated supersymmetry breaking (AMSB) effect [35, 36] violates SUSY and R symmetry simultaneously, and it can be formulated by the Weyl compensator $\Phi = 1 + \theta^2 m_{3/2}$ [37] as

$$\mathcal{L} = \int d^2\theta \Phi \Phi^* K + \left[\int d^2\theta \Phi^3 W + \text{h.c.} \right]. \quad (2.16)$$

At tree level, we obtain

$$\mathcal{L}_{\text{AMSB}} = m_{3/2} \left(-3W + \sum_i \phi_i \frac{\partial W}{\partial \phi_i} \right) + \text{h.c.} \quad (2.17)$$

This effect is phenomenologically important for gaugino masses and also the mass of R -axion. Note that the VEVs given in eq. (2.14) are not affected as long as $m_{3/2} \ll m$. In the limit of $m_{3/2} \gg m$, the VEVs of \bar{F}_q , $\bar{F}_{\bar{q}}$, and A become close to the vacuum obtained in Ref. [23].

In the limit of $\alpha_{\text{SU}(N)_2} = 0$ and $m_{3/2} = 0$, the chiral Lagrangian based on $\text{SU}(2N)_{\bar{F}} \times \text{U}(1)_{\text{PQ}} \times \text{U}(1)_R / \text{Sp}(2N)_{\bar{F}}$ provides a low energy effective description. The total number of NG bosons is $2N^2 - N + 1$. It includes $2N^2 - N - 1$ NG bosons from $\text{SU}(2N)_{\bar{F}} / \text{Sp}(2N)_{\bar{F}}$, a PQ-axion, and an R -axion. Note that NG bosons in $\text{SU}(2N)_{\bar{F}} / \text{Sp}(2N)_{\bar{F}}$ are described as \square of $\text{Sp}(2N)_{\bar{F}}$. Thus, NG bosons from $\text{SU}(2N)_{\bar{F}} \times \text{U}(1)_{\text{PQ}} \times \text{U}(1)_R / \text{Sp}(2N)_{\bar{F}}$ can be understood as

$$\left[\square \oplus \mathbf{1} \oplus \mathbf{1} \right]_{\text{Sp}(2N)_{\bar{F}}} = \left[\square \oplus \bar{\square} \oplus \mathbf{adj} \oplus \mathbf{1} \oplus \mathbf{1} \right]_{\text{SU}(N)_d}. \quad (2.18)$$

$\text{SU}(N)_d$ gauge interaction explicitly violates the shift symmetry for those modes and the radiative correction induces their masses $m^2 \sim \alpha_{\text{SU}(N)_d} \phi^2$ [13, 38]. Then, the light bosons whose masses are much smaller than ϕ are PQ-axion and R -axion.

The mass of R -axion is induced by an explicit R symmetry breaking. By using $W \sim \Lambda_{\text{Sp}(4)}^3$, we obtain the mass of R -axion as

$$m_R^2 \sim \frac{m_{3/2} \Lambda_{\text{Sp}(4)}^3}{\phi^2} \sim m_{3/2} m. \quad (2.19)$$

Let us discuss the domain wall number N_{DW} in the current model. $\text{U}(1)_{\text{PQ}}$ transformation is given as

$$\bar{F}_q \rightarrow \bar{F}_q \exp(i(N+1)\alpha), \quad \bar{F}_{\bar{q}} \rightarrow \bar{F}_{\bar{q}} \exp(i(N+1)\alpha), \quad A \rightarrow A \exp(-iN\alpha). \quad (2.20)$$

We define the anomaly coefficient of $\text{U}(1)_{\text{PQ}}\text{-SU}(N)_2\text{-SU}(N)_2$ as

$$N_{\text{anom}} = \left| \sum_{\Phi} 2Q_{\Phi} d_{\Phi} \right|, \quad (2.21)$$

where Q_{Φ} and d_{Φ} is the PQ charge and the Dynkin index of $\text{SU}(N)_2$ representation of a chiral superfield Φ . We take the normalization for fundamental representation to be $d = 1/2$. Then, the anomaly coefficient is

$$N_{\text{anom}} = \underbrace{(N+1)(2N+4)}_{\bar{F}_q} + \underbrace{(N+1)(2N+4)}_{\bar{F}_{\bar{q}}} = 4(N+1)(N+2). \quad (2.22)$$

$\text{SU}(2N+4)_1$ gauge group has its center Z_{2N+4} and it works as

$$\bar{F}_q \rightarrow \bar{F}_q \exp\left(\frac{-2\pi i k}{2N+4}\right), \quad \bar{F}_{\bar{q}} \rightarrow \bar{F}_{\bar{q}} \exp\left(\frac{-2\pi i k}{2N+4}\right), \quad A \rightarrow A \exp\left(\frac{4\pi i k}{2N+4}\right), \quad (2.23)$$

where k is an integer. We can see that $\text{U}(1)_{\text{PQ}}$ with $\alpha = 2\pi/(N+2)$ and Z_{2N+4} with $k = 2$ are equivalent. Thus, to count the number of degenerated vacua N_{DW} , the vacua connected by a gauge transformation should be regarded as the same vacuum [39], and we obtain

$$N_{\text{DW}} = \frac{N_{\text{anom}}}{N+2} = 4(N+1). \quad (2.24)$$

Now let us discuss the effective axion decay constant. By parametrizing $\bar{F}_q = \langle \bar{F}_q \rangle \exp(i(N+1)\theta)$, $\bar{F}_{\bar{q}} = \langle \bar{F}_{\bar{q}} \rangle \exp(i(N+1)\theta)$, and $A = \langle A \rangle \exp(-iN\theta)$, the effective Lagrangian of θ is

$$\mathcal{L} = \left(2N(N+1)^2\phi^2 + 2c^2N^3 + 4c'^2N^2 \right) (\partial_{\mu}\theta)^2 + \frac{N_{\text{anom}}\theta}{32\pi^2} G_{\mu\nu} \tilde{G}^{\mu\nu}. \quad (2.25)$$

We define the canonically normalized axion field a as

$$a \equiv \sqrt{4N(N+1)^2\phi^2 + 4c^2N^3 + 8c'^2N^2} \times \theta, \quad (2.26)$$

and obtain the following effective Lagrangian:

$$\mathcal{L} = \frac{1}{2}(\partial_{\mu}a)^2 + \frac{a}{f_a} \frac{1}{32\pi^2} G_{\mu\nu} \tilde{G}^{\mu\nu}, \quad (2.27)$$

where the decay constant f_a is defined as

$$f_a = \frac{\sqrt{4N(N+1)^2\phi^2 + 4c^2N^3 + 8c'^2N^2}}{N_{\text{anom}}} = w_N \Lambda_{2N+4} \left(\frac{\Lambda_{2N+4}}{m} \right)^{3/(4N+8)}. \quad (2.28)$$

w_N is coefficient determined by N . For its numerical value, see Tab. 2.

	$SU(2N-4)_1$	$SU(N)_2$	$U(1)_{PQ}$	$U(1)_q$	$U(1)_R$	$SU(2N)_{\bar{F}}$
\bar{F}_q	\square	\square	$2N-2$	1	0	\square
$\bar{F}_{\bar{q}}$	\square	\square	$2N-2$	-1	0	
S	$\square\square$	$\mathbf{1}$	$-2N$	0	$3/(N-1)$	$\mathbf{1}$

Table 3. Matter content of SUSY Bars-Yankielowicz model.

	$SO(8)$	$SU(N)_2$	$U(1)_{PQ}$	$U(1)_q$	$U(1)_R$	$SU(2N)_{\bar{F}}$
q	$\mathbf{8}_v$	\square	$-N+2$	1	$(2N-5)/(2N-2)$	\square
\bar{q}	$\mathbf{8}_v$	\square	$-N+2$	-1	$(2N-5)/(2N-2)$	
p	$\mathbf{8}_s$	$\mathbf{1}$	$2N(N-2)$	0	$-(2N-5)/(N-1)$	$\mathbf{1}$
M	$\mathbf{1}$	$\square\square$	$2N-4$	2	$3/(N-1)$	$\square\square$
\bar{M}	$\mathbf{1}$	$\square\square$	$2N-4$	-2	$3/(N-1)$	
M_a	$\mathbf{1}$	\mathbf{adj}	$2N-4$	0	$3/(N-1)$	
M_s	$\mathbf{1}$	$\mathbf{1}$	$2N-4$	0	$3/(N-1)$	
U	$\mathbf{1}$	$\mathbf{1}$	$-4N(N-2)$	0	$6(N-2)/(N-1)$	$\mathbf{1}$

Table 4. Matter content of magnetic theory of SUSY Bars-Yankielowicz model. Note that $\mathbf{8}_v$ and $\mathbf{8}_s$ are vector and spinor representation of $SO(8)$.

2.2 Axion from SUSY Bars-Yankielowicz type model

Let us discuss another example of chiral gauge theory having an axion. We introduce $SU(2N-4)_1 \times SU(N)_2$ gauge symmetry and chiral multiplets \bar{F}_q (\square, \square), $\bar{F}_{\bar{q}}$ (\square, \square), and S ($\square\square, \mathbf{1}$). Here we utilize the analysis presented in Ref. [24] and assume $N \geq 9$ to have spontaneous breaking of global symmetries. We assume that the dynamical scale of $SU(N)_2$ gauge symmetry is much lower than that of $SU(2N-4)_1$ gauge symmetry, i.e., $\Lambda_N \ll \Lambda_{2N-4}$. We can find $U(1)_{PQ} \times U(1)_q \times U(1)_R$ global symmetries, which are free from $SU(2N-4)_1$ anomaly. The matter content is summarized in Tab. 3. We choose the charge assignment of $U(1)_q$ and $U(1)_R$ such that both $U(1)_q$ and $U(1)_R$ are free from $SU(N)_2$ anomaly. We assume $W_{\text{tree}} = 0$. Note that $SU(2N)_{\bar{F}}$ global symmetry arises in the limit of $\Lambda_N \rightarrow 0$ and this $SU(2N)_{\bar{F}}$ global symmetry is equivalent to that of Ref. [24]. $SU(N)_2 \times U(1)_q$ can be understood as a subgroup of $SU(2N)_{\bar{F}}$.

The low energy degrees of freedom of this model can be described by a magnetic dual [24, 40]. The magnetic description is given by $SO(8)$ gauge theory. Its matter content is summarized in Tab. 4. The magnetic theory has the following superpotential:

$$W_{\text{mag,tree}} = y_M(\tilde{M}qq + \tilde{M}\bar{q}\bar{q} + \tilde{M}_aq\bar{q} + \tilde{M}_s\bar{q}q) + y_U\tilde{U}pp. \quad (2.29)$$

Note that \tilde{M} and \tilde{U} are normalized such that they have canonical Kähler potential. We assume $y_M \sim y_U \sim 4\pi$ from naive dimensional analysis [41, 42]. After q , \bar{q} , and p are integrated out, the magnetic theory becomes pure $SO(8)$ SUSY Yang-Mills theory, and its dynamical scale $\tilde{\Lambda}_L$ is determined as

$$\tilde{\Lambda}_L^{18} = \frac{y_M^{2N} y_U \det \tilde{\mathcal{M}} \tilde{U}}{\tilde{\Lambda}^{2N-17}}, \quad (2.30)$$

where $\tilde{\mathcal{M}}$ is defined as

$$\tilde{\mathcal{M}} = \begin{pmatrix} \tilde{M} & \tilde{M}_a + \tilde{M}_s \\ (\tilde{M}_a + \tilde{M}_s)^T & \tilde{M} \end{pmatrix}. \quad (2.31)$$

Thus, we obtain the dynamical superpotential as [43]

$$W_{\text{mag,dyn}} \sim \left(\frac{y_M^{2N} y_U \det \tilde{\mathcal{M}} \tilde{U}}{\tilde{\Lambda}^{2N-17}} \right)^{1/6}. \quad (2.32)$$

Here we assume SUSY breaking effect is dominated by the AMSB effect for simplicity of analysis. Let us introduce the Weyl compensator $\Phi = 1 + \theta^2 m_{3/2}$ [37] as

$$\begin{aligned} \mathcal{L}_{\text{AMSB}} &= m_{3/2} \left(-3W_{\text{mag,dyn}} + \sum_{\phi_i} \phi_i \frac{\partial W_{\text{mag,dyn}}}{\partial \phi_i} \right) + \text{h.c.} \\ &\sim m_{3/2} \left(\frac{2N-17}{6} \right) W_{\text{mag,dyn}} + \text{h.c.} \end{aligned} \quad (2.33)$$

We can find the vacuum is stabilized at

$$\tilde{M}_s \sim m_{3/2} \left(\frac{\tilde{\Lambda}}{m_{3/2}} \right)^{(2N-17)/(2N-11)}, \quad \tilde{U} \sim m_{3/2} \left(\frac{\tilde{\Lambda}}{m_{3/2}} \right)^{(2N-17)/(2N-11)}. \quad (2.34)$$

These VEVs are smaller than $\tilde{\Lambda}$ and it justifies our weakly coupled analysis in the magnetic theory. Note that this vacuum is deeper than the vacuum around the origin of $\tilde{\mathcal{M}}$ and \tilde{U} as discussed in Ref. [24].

The chiral Lagrangian based on $\text{SU}(2N)_{\bar{F}} \times \text{U}(1)_{\text{PQ}} \times \text{U}(1)_R / \text{SO}(2N)_{\bar{F}}$ provides a low energy effective description. The total number of NG bosons is $2N^2 + N + 1$, and it includes $2N^2 + N - 1$ NG bosons from $\text{SU}(2N)_{\bar{F}} / \text{SO}(2N)_{\bar{F}}$ are described as $\square\square$ of $\text{SO}(2N)_{\bar{F}}$.

$$\left[\square\square \oplus \mathbf{1} \oplus \mathbf{1} \right]_{\text{SO}(2N)_{\bar{F}}} = \left[\square\square \oplus \overline{\square\square} \oplus \mathbf{adj} \oplus \mathbf{1} \oplus \mathbf{1} \right]_{\text{SU}(N)_{\bar{d}}}. \quad (2.35)$$

$\text{SU}(N)_d$ gauge interaction explicitly violates the shift symmetry for those modes and the radiative correction induces their masses $m^2 \sim \alpha_{\text{SU}(N)_d} \langle \tilde{M} \rangle^2$ [13, 38]. Then, the light bosons whose masses are much smaller than $\langle \tilde{M} \rangle$ are PQ-axion and R -axion. The mass of R -axion is estimated as

$$m_R^2 \sim m_{3/2} \tilde{\Lambda}_L^3 \left[m_{3/2} \left(\frac{\tilde{\Lambda}}{m_{3/2}} \right)^{(2N-17)/(2N-11)} \right]^{-2} \sim m_{3/2}^2. \quad (2.36)$$

Let us discuss the anomaly coefficient N_{anom} and the number of physical vacua N_{DW} in the current model. In the electric theory, $\text{U}(1)_{\text{PQ}}$ transformation is given as

$$\bar{F}_q \rightarrow \bar{F}_q \exp(i(2N-2)\alpha), \quad \bar{F}_{\bar{q}} \rightarrow \bar{F}_{\bar{q}} \exp(i(2N-2)\alpha), \quad S \rightarrow S \exp(-2iN\alpha). \quad (2.37)$$

Then, the anomaly coefficient is

$$N_{\text{anom}}^{(\text{ele})} = \underbrace{(2N-2)(2N-4)}_{\bar{F}_q} + \underbrace{(2N-2)(2N-4)}_{\bar{F}_{\bar{q}}} = 8(N-1)(N-2). \quad (2.38)$$

$\text{SU}(2N-4)_1$ gauge group has the center Z_{2N-4} and it works as

$$\bar{F}_q \rightarrow \bar{F}_q \exp\left(\frac{-2\pi i k}{2N-4}\right), \quad \bar{F}_{\bar{q}} \rightarrow \bar{F}_{\bar{q}} \exp\left(\frac{-2\pi i k}{2N-4}\right), \quad A \rightarrow A \exp\left(\frac{4\pi i k}{2N-4}\right), \quad (2.39)$$

where k is an integer. Therefore we can see that $\text{U}(1)_{\text{PQ}}$ with $\alpha = \pi/(N-2)$ and Z_{2N-4} with $k = -2$ are equivalent. Thus, to count the number of degenerated vacua $N_{\text{vac}}^{(\text{ele})}$ in the electric theory, the vacua connected by a gauge transformation should be regarded as the same vacuum [39], and we obtain

$$N_{\text{DW}}^{(\text{ele})} = \frac{N_{\text{anom}}^{(\text{ele})}}{2(N-2)} = 4(N-1). \quad (2.40)$$

In the magnetic theory, $\text{U}(1)_{\text{PQ}}$ transformation is given as

$$q \rightarrow q \exp(-i(N-2)\alpha), \quad p \rightarrow p \exp(2iN(N-2)\alpha), \quad M \rightarrow M \exp(2i(N-2)\alpha). \quad (2.41)$$

The anomaly coefficient is

$$\begin{aligned} N_{\text{anom}}^{(\text{mag})} &= \underbrace{8(-N+2)}_q + \underbrace{8(-N+2)}_{\bar{q}} + \underbrace{(2N-4)(N+2)}_M + \underbrace{(2N-4)(N+2)}_{\bar{M}} + \underbrace{(2N-4)2N}_{M_a} \\ &= 8(N-1)(N-2). \end{aligned} \quad (2.42)$$

We can find a center $Z_2 \in \text{Spin}(8)$ which works as

$$q \rightarrow -q, \quad p \rightarrow p. \quad (2.43)$$

Thus, $\text{U}(1)_{\text{PQ}}$ transformation with $\alpha = \pi/(N-2)$ can be identified with this Z_2 . Then, the number of vacua in the magnetic theory is

$$N_{\text{DW}}^{(\text{mag})} = \frac{N_{\text{anom}}^{(\text{mag})}}{2(N-2)} = 4(N-1). \quad (2.44)$$

$N_{\text{anom}}^{(\text{ele})} = N_{\text{anom}}^{(\text{mag})}$ can be regarded as one of anomaly matching condition between electric theory and magnetic theory. Since $N_{\text{DW}}^{(\text{ele})} = N_{\text{DW}}^{(\text{mag})}$ is satisfied, the number of degenerated vacua is also consistent.

	$SU(14)_1$	$SU(5)_2$	$U(1)_{PQ}$	$U(1)_q$	$SU(10)_{\bar{F}}$
\bar{F}_q	\square	\square	6	1	\square
$\bar{F}_{\bar{q}}$	\square	\square	6	-1	
A	\square	$\mathbf{1}$	-5	0	$\mathbf{1}$
$\Phi = (\bar{D} \oplus L)$	$\mathbf{1}$	\square	0	0	$\mathbf{1}$
$\Psi = (Q \oplus \bar{U} \oplus \bar{E})$	$\mathbf{1}$	\square	0	0	$\mathbf{1}$
H	$\mathbf{1}$	\square	0	0	$\mathbf{1}$
\bar{H}	$\mathbf{1}$	\square	0	0	$\mathbf{1}$
Σ	$\mathbf{1}$	\mathbf{adj}	0	0	$\mathbf{1}$

Table 5. Matter content of a GUT motivated QCD axion model.

2.3 Generalization of axion models

So far, we have discussed two simple examples of the axion model; the SUSY Georgi-Glashow type model and the SUSY Bars-Yankielowicz type model. In both models, we identify \bar{F} as $\square + \bar{\square}$ of $SU(N)_2$ gauge theory. We can easily modify this setup by considering other representations of gauge group. For example, if we only gauge $SU(m)$ which is a subgroup of $SU(N)$, we can construct a Georgi-Glashow type model with $SU(2N+4)_1 \times SU(m)_1$ gauge symmetry and chiral multiplets $(\bar{\square}, \square) + (\bar{\square}, \bar{\square}) + (2N-2m)(\bar{\square}, \mathbf{1}) + (\square, \mathbf{1})$. Another possibility is introducing larger $SU(N)_2$ representation such as \mathbf{adj} . As in discussion so far, the low energy degrees of freedom in those models can be analyzed by using chiral Lagrangian with gauge symmetry as well.

3 GUT-motivated QCD axion model

In this section, we construct a QCD axion model which is based on the SUSY Georgi-Glashow type model with $N = 5$. This is a minimal setup with $SU(5)$ GUT which is based on the discussions in the previous section. The model has $SU(14)_1 \times SU(5)_2$ gauge symmetry and chiral multiplets \bar{F}_q $(\bar{\square}, \square)$, $\bar{F}_{\bar{q}}$ $(\bar{\square}, \bar{\square})$, and A $(\square, \mathbf{1})$. We introduce MSSM chiral multiplets as $SU(5)_2$ charged multiplets. Φ $(\mathbf{1}, \bar{\square})$ behaves as \bar{D} and L , Ψ $(\mathbf{1}, \square)$ behaves as Q , \bar{U} , and \bar{E} . The Higgs doublets H_u and H_d come from H $(\mathbf{1}, \square)$ and \bar{H} $(\mathbf{1}, \bar{\square})$. Σ $(\mathbf{1}, \mathbf{adj})$ is introduced to break $SU(5)_2$ gauge symmetry by its VEV¹,

$$\langle \Sigma \rangle = \sigma \text{diag}(2, 2, 2, -3, -3). \quad (3.1)$$

The matter content and charge assignments are summarized in Tab. 5. We assume that the dynamical scale of $SU(5)_2$ gauge symmetry is much below than that of $SU(14)_1$ gauge symmetry, i.e., $\Lambda_5 \ll \Lambda_{14}$. The standard model gauge group $SU(3)_c \times SU(2)_L \times U(1)_Y$ can be understood as a subgroup of $SU(5)_{\text{GUT}}$, which is the diagonal subgroup of $SU(5)_1 \subset SU(14)_1$ and $SU(5)_2$.

In the following of this paper, we assume mini-split SUSY like SUSY breaking [44–50]; sfermions obtain their mass from $K \sim Z^\dagger Z Q Q^\dagger / M_{\text{pl}}^2$ as $m^2 = F_Z^2 / M_P^2 = \mathcal{O}((100 \text{ TeV})^2)$,

¹ Σ is normalized to have its Kähler potential as $K = \text{tr}[\Sigma^\dagger \Sigma]$.

and the gauginos obtain from AMSB effect [35, 36] as $m_{1/2} = \mathcal{O}(1 \text{ TeV})$. The axion decay constant f_a and the dynamical scale of $\text{Sp}(4)$ $\Lambda_{\text{Sp}(4)}$ can be written as functions of Λ_{14} and m by using eq. (2.28) and eq. (2.15) as

$$f_a = w_5 \Lambda_{14} \left(\frac{\Lambda_{14}}{m} \right)^{3/28}, \quad \Lambda_{\text{Sp}(4)} = z_5 \Lambda_{14} \left(\frac{\Lambda_{14}}{m} \right)^{-11/42}. \quad (3.2)$$

For the numerical value of w_5 and z_5 , see Tab. 2.

3.1 Symmetry breaking scale and VEVs

In the current model, we have two symmetry breaking scales; the PQ breaking scale M_{PQ} and the GUT scale M_{GUT} . Those two scales are determined by two VEVs of chiral multiplets. One is the VEV ϕ in \bar{F}_q and $\bar{F}_{\bar{q}}$, and A given in eq. (2.4) and this is responsible for the PQ breaking. The other one is σ in the VEV of Σ given in eq. (3.1) and this is responsible for $\text{SU}(5)_{2/\text{GUT}}$ gauge symmetry breaking. In this subsection, we outline how M_{PQ} , M_{GUT} , ϕ , and σ are related to Λ_{14} .

In our analysis, we treat M_{PQ} and M_{GUT} as energy scales at which the RG running of couplings changes. For given M_{PQ} , we can determine M_{GUT} from the following procedure. M_{GUT} is determined as a scale at which two gauge couplings unify. Suppose that there exists a solution of $M_{\text{GUT}} < M_{\text{PQ}}$ such that

$$\alpha_a(M_{\text{GUT}}) = \alpha_b(M_{\text{GUT}}). \quad (3.3)$$

Here $\alpha_{1,2,3}$ are the gauge coupling of $\text{SU}(3)_c \times \text{SU}(2)_L \times \text{U}(1)_Y$. For this definition, there are three possible choices of (a, b) as $(1, 2)$, $(2, 3)$, and $(3, 1)$. In this case, the symmetry breaking pattern from UV to IR is as follows:

$$\begin{aligned} & [\text{SU}(14)_1 \times \text{SU}(5)_2] \times \text{U}(1)_{\text{PQ}} \times \text{U}(1)_q \times \text{U}(1)_R \\ \rightarrow & [\text{Sp}(4)_1 \times \text{SU}(5)_{\text{GUT}}] \times \text{U}(1)_d \\ \rightarrow & [\text{Sp}(4)_1 \times \text{SU}(3)_c \times \text{SU}(2)_L \times \text{U}(1)_Y] \times \text{U}(1)_d. \end{aligned} \quad (3.4)$$

If there is no solution of $M_{\text{GUT}} < M_{\text{PQ}}$ in eq. (3.3), the GUT scale should be above the PQ breaking scale, i.e., $M_{\text{GUT}} > M_{\text{PQ}}$. In this case, the symmetry breaking pattern from UV to IR is

$$\begin{aligned} & [\text{SU}(14)_1 \times \text{SU}(5)_2] \times \text{U}(1)_{\text{PQ}} \times \text{U}(1)_q \times \text{U}(1)_R \\ \rightarrow & [\text{SU}(14)_1 \times \text{SU}(3)_2 \times \text{SU}(2)_2 \times \text{U}(1)_2] \times \text{U}(1)_{\text{PQ}} \times \text{U}(1)_q \times \text{U}(1)_R \\ \rightarrow & [\text{Sp}(4)_1 \times \text{SU}(3)_c \times \text{SU}(2)_L \times \text{U}(1)_Y] \times \text{U}(1)_d, \end{aligned} \quad (3.5)$$

and we take a tree level matching condition at M_{PQ} as

$$\begin{aligned} \frac{1}{\alpha_1(M_{\text{PQ}})} &= \frac{1}{\tilde{\alpha}_1(M_{\text{PQ}})} + \frac{1}{\alpha_{14}(M_{\text{PQ}})}, \\ \frac{1}{\alpha_2(M_{\text{PQ}})} &= \frac{1}{\tilde{\alpha}_2(M_{\text{PQ}})} + \frac{1}{\alpha_{14}(M_{\text{PQ}})}, \\ \frac{1}{\alpha_3(M_{\text{PQ}})} &= \frac{1}{\tilde{\alpha}_3(M_{\text{PQ}})} + \frac{1}{\alpha_{14}(M_{\text{PQ}})}. \end{aligned} \quad (3.6)$$

Here $\tilde{\alpha}_{1,2,3}$ are the gauge coupling of $SU(3)_2 \times SU(2)_2 \times U(1)_2 (\subset SU(5)_2)$ and α_{14} is the gauge coupling of $SU(14)_1$. Then, M_{GUT} is determined from

$$\tilde{\alpha}_a(M_{\text{GUT}}) = \tilde{\alpha}_b(M_{\text{GUT}}). \quad (3.7)$$

From this procedure, we can determine M_{GUT} as a function of M_{PQ} . Same as eq. (3.3), there are three possible choices of (a, b) in eq. (3.7) as $(1, 2)$, $(2, 3)$, and $(3, 1)$.

For given M_{PQ} and M_{GUT} , we can determine the VEVs ϕ and σ as follows. As discussed in appendix B, the gauge couplings of UV and IR theories are matched at the scale of the mass of massive gauge bosons. Thus, we determine ϕ as

$$\phi = \begin{cases} [\tilde{g}_c^2(M_{\text{PQ}}) + g_{14}^2(M_{\text{PQ}})]^{-1/2} M_{\text{PQ}} & (M_{\text{PQ}} < M_{\text{GUT}}) \\ [(g_5^2(M_{\text{PQ}}) + g_{14}^2(M_{\text{PQ}}))]^{-1/2} M_{\text{PQ}} & (M_{\text{PQ}} > M_{\text{GUT}}) \end{cases} \quad (3.8)$$

The possible choices of c are $c = a$ or $c = b$, and then ϕ behaves as a continuous function of M_{PQ} at $M_{\text{PQ}} = M_{\text{GUT}}$. We can also apply a similar discussion to σ if there is a large hierarchy between M_{PQ} and M_{GUT} . For $M_{\text{PQ}} \gg M_{\text{GUT}}$, the VEV of Σ given in eq. (3.1) breaks the $SU(5)_2$ into $SU(3)_2 \times SU(2)_2 \times U(1)_2$ gauge group. Thus, the GUT scale can be understood as $M_{\text{GUT}} = 5\sqrt{2}g_5\sigma$. On the other hand, in the case of $M_{\text{PQ}} \ll M_{\text{GUT}}$, the GUT scale can be understood as $M_{\text{GUT}} = 5\sqrt{2}g_{\text{GUT}}\sigma$. For these cases, we extract σ as

$$\sigma = \begin{cases} (5\sqrt{2}g_5)^{-1}M_{\text{GUT}} & (M_{\text{PQ}} \ll M_{\text{GUT}}) \\ (5\sqrt{2}g_{\text{GUT}})^{-1}M_{\text{GUT}} & (M_{\text{PQ}} \gg M_{\text{GUT}}) \end{cases} \quad (3.9)$$

See appendix B for more details including the case with $M_{\text{PQ}} \simeq M_{\text{GUT}}$. Eq. (2.14) gives us the relation between ϕ and Λ_{14} . By using the above discussion, M_{GUT} , ϕ , and σ can be expressed as functions of M_{PQ} . Thus, by solving these relations for Λ_{14} , we can express M_{PQ} , M_{GUT} , ϕ , and σ as functions of Λ_{14} .

Let us comment on the choice of (a, b, c) in eq. (3.3), eq. (3.7), and eq. (3.8). To evaluate M_{GUT} and ϕ , we have the following six choices for (a, b, c) :

- $(a, b, c) = (1, 2, 1)$
- $(a, b, c) = (1, 2, 2)$
- $(a, b, c) = (2, 3, 2)$
- $(a, b, c) = (2, 3, 3)$
- $(a, b, c) = (3, 1, 3)$
- $(a, b, c) = (3, 1, 1)$

The different choices of (a, b) in eq. (3.3) and eq. (3.7) may lead to different M_{GUT} and we expect the effect of this difference should be similar to the threshold correction from the particles at the GUT scale. Also the effect of the difference between the choices of c should be similar to the threshold corrections at the PQ breaking scale. In our analysis, we

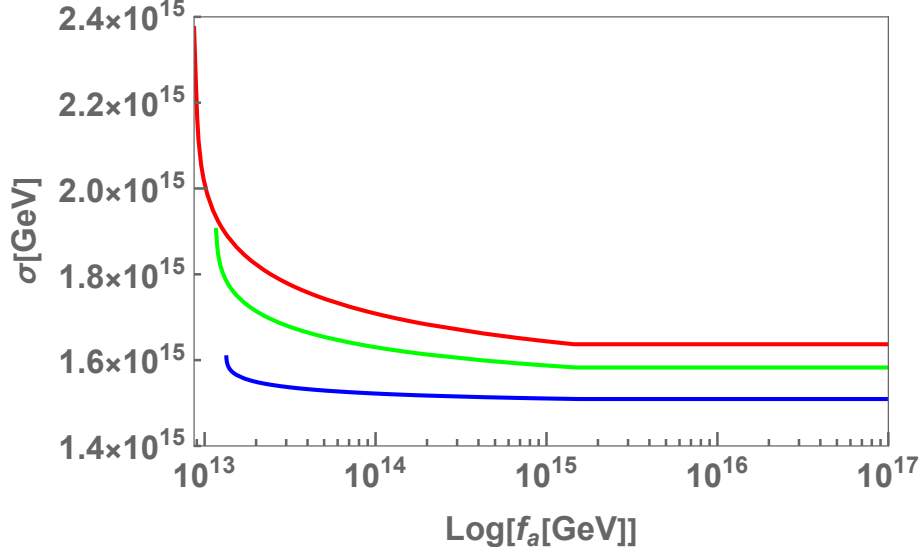


Figure 1. This plot shows the GUT breaking VEV σ as a function of the axion decay constant f_a . Red, blue, and green solid curves indicate the results for $(a, b, c) = (1, 2, 2)$, $(2, 3, 3)$, and $(3, 1, 3)$, respectively.

are agnostic about the threshold correction, and we estimate an uncertainty of threshold correction from the difference among the choices of (a, b, c) . We will see that the choice of (a, b, c) affects the estimation of the proton lifetime in section 3.3.

At the end of this subsection, we show the GUT breaking VEV σ as a function of the axion decay constant f_a in figure 1. Here we estimate the GUT scale as $\alpha_a(M_{\text{GUT}}) = \alpha_b(M_{\text{GUT}})$ for $(a, b) = (1, 2)$, $(2, 3)$, $(3, 1)$, and take c to be higher PQ breaking scale in the choice of (a, b) . Then, the red, blue, and green curves in figure 1 indicate the results for $(a, b, c) = (1, 2, 2)$, $(2, 3, 3)$, and $(3, 1, 3)$, respectively. In the case of $M_{\text{PQ}} > M_{\text{GUT}}$, this is the same as the minimal SU(5) GUT. Therefore, the GUT breaking VEV σ is independent of f_a . On the other hand, in the case of $M_{\text{PQ}} < M_{\text{GUT}}$, the GUT breaking VEV σ becomes larger for lower f_a . The behavior of σ connects smoothly including in the case of $M_{\text{PQ}} \simeq M_{\text{GUT}}$. See appendix B for the details of the derivation of the GUT breaking VEV σ . For each curve, there is a lowerbound on f_a to avoid the appearance of a Landau pole below the GUT scale. See also a discussion in section 3.3.

3.2 Numerical analysis of coupling unification

In this subsection, we show a numerical analysis of the renormalization group (RG) running of the gauge couplings in the current model. As we have discussed so far, the symmetry breaking pattern from UV to IR and the RG running of the gauge couplings depend on the hierarchy between M_{PQ} and M_{GUT} . The relevant RG equations for both $M_{\text{PQ}} < M_{\text{GUT}}$ and $M_{\text{PQ}} > M_{\text{GUT}}$ are summarized in appendix C. As we will see in this section, the PQ breaking scale cannot be arbitrary low for successful GUT unification.

For our analysis, we discuss the RG running of the gauge couplings at two-loop level and the top Yukawa coupling y_t at one-loop level. We neglect other Yukawa couplings.

We take the SM input parameters g' , g_2 , g_3 , and y_t at $\mu = 200$ GeV in the $\overline{\text{MS}}$ scheme from Ref. [51], and calculate the coupling constants in the $\overline{\text{DR}}$ scheme. For details, see appendix C.1. For the MSSM parameter, we take the wino mass $M_{\tilde{W}} = 3$ TeV, the ratio of gluino and wino mass $M_{\tilde{g}}/M_{\tilde{W}} = 9$, the remaining sfermions and heavy Higgs masses to be $M_S = 100$ TeV, and $\tan\beta = 3$.

3.2.1 The case of $M_{\text{PQ}} > M_{\text{GUT}}$

First, let us consider the case of $M_{\text{PQ}} > M_{\text{GUT}}$. The symmetry breaking pattern from UV to IR is given in eq. (3.4). At $200 \text{ GeV} < \mu < M_2$, the RG running of couplings is described by the SM beta functions given in [52, 53]. Then, the SM and the SM with gauginos is matched at $\mu = M_2$ by taking care of the one-loop threshold correction [54]. At $M_2 < \mu < M_S$, the RG running is described by the SM + gaugino beta functions in [54]. At $M_S < \mu < M_{\text{GUT}}$, the RG running is described by the MSSM beta functions in eqs. (C.3, C.5). At the GUT scale M_{GUT} , $\langle \Sigma \rangle$ breaks $\text{SU}(5)_{\text{GUT}}$ gauge group into the SM gauge group as

$$\text{SU}(5)_{\text{GUT}} \rightarrow \text{SU}(3)_c \times \text{SU}(2)_L \times \text{U}(1)_Y. \quad (3.10)$$

The tree level matching condition is given as

$$\frac{1}{\alpha_a(M_{\text{GUT}})} = \frac{1}{\alpha_b(M_{\text{GUT}})} = \frac{1}{\alpha_{\text{GUT}}(M_{\text{GUT}})}. \quad (3.11)$$

Here, α_{GUT} is the gauge coupling for $\text{SU}(5)_{\text{GUT}}$. The beta functions at $M_{\text{GUT}} < \mu < M_{\text{PQ}}$ are given in eqs. (C.6, C.8). At the PQ breaking scale, the gauge symmetry is spontaneously broken as

$$\text{SU}(5)_1 \times \text{SU}(5)_2 \rightarrow \text{SU}(5)_{\text{GUT}}. \quad (3.12)$$

Then, the tree level matching condition is given as

$$\frac{1}{\alpha_{\text{GUT}}(M_{\text{PQ}})} = \frac{1}{\alpha_5(M_{\text{PQ}})} + \frac{1}{\alpha_{14}(M_{\text{PQ}})}. \quad (3.13)$$

The beta functions at $\mu > M_{\text{PQ}}$ are given in eqs. (C.12, C.14).

Figure 2 shows an example of successful GUT unification. We take the dynamical scale of $\text{SU}(14)_1$ gauge group as $\Lambda_{14} = 10^{16}$ GeV, and the GUT scale for the case of $(a, b) = (1, 2)$. The SM gauge couplings are unified successfully at the GUT scale, which is depicted by vertical brown dashed line. Above that scale, the unified gauge coupling is changed to satisfy the matching conditions eq. (3.13) at the PQ breaking scale, which is denoted by vertical black dashed line.

3.2.2 The case of $M_{\text{PQ}} < M_{\text{GUT}}$

Next, let us consider the case of $M_{\text{PQ}} < M_{\text{GUT}}$. The symmetry breaking pattern from UV to IR is given in eq. (3.5). The RG running and threshold correction of couplings from 200 GeV to M_S are the same as the case of $M_{\text{PQ}} > M_{\text{GUT}}$. The beta functions

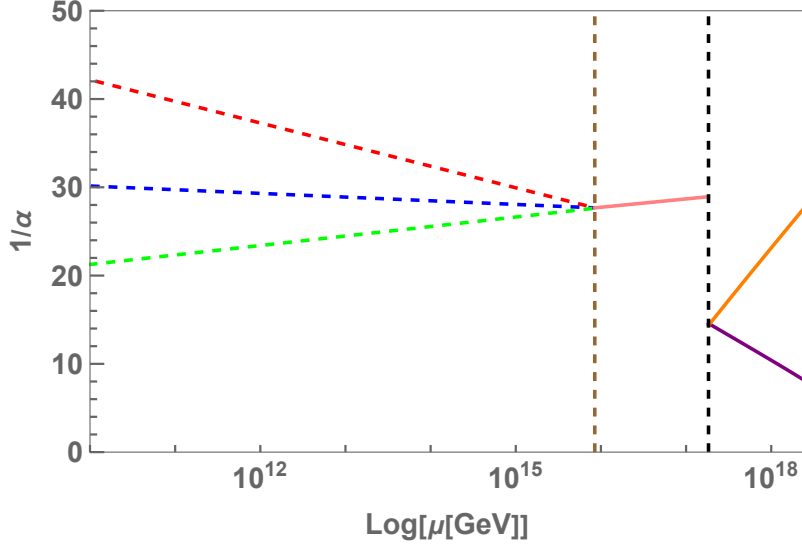


Figure 2. The RG running of gauge couplings with $M_{\text{PQ}} > M_{\text{GUT}}$, $\Lambda_{14} = 10^{16}$ GeV, and $(a, b) = (1, 2)$. The red, blue, and green dashed lines show the SM gauge couplings, α_1 , α_2 , and α_3 , while the purple and orange solid lines denote α_5 and α_{14} , which are the gauge couplings of $\text{SU}(5)_2$ and $\text{SU}(14)_1$, respectively. The pink solid line shows the running of the unified coupling α_{GUT} . The vertical black and brown dashed lines depict the PQ breaking and GUT scale, respectively. We set the MSSM particle mass as wino mass $M_{\tilde{W}} = 3$ TeV, the ratio of gluino and wino mass $M_{\tilde{g}}/M_{\tilde{W}} = 9$, the remaining sparticle mass $M_S = 100$ TeV, and $\tan \beta = 3$.

at $M_S < \mu < M_{\text{PQ}}$ are given by eqs. (C.3, C.5). At the PQ breaking scale, the gauge symmetry is spontaneously broken by the VEV of \bar{F}_q and $\bar{F}_{\bar{q}}$ as

$$\text{SU}(3)_1 \times \text{SU}(3)_2 \rightarrow \text{SU}(3)_c, \quad (3.14)$$

$$\text{SU}(2)_1 \times \text{SU}(2)_2 \rightarrow \text{SU}(2)_L, \quad (3.15)$$

$$\text{U}(1)_1 \times \text{U}(1)_2 \rightarrow \text{U}(1)_Y. \quad (3.16)$$

Then, the tree level matching conditions at $\mu = M_{\text{PQ}}$ are given as

$$\begin{aligned} \frac{1}{\alpha_1(M_{\text{PQ}})} &= \frac{1}{\tilde{\alpha}_1(M_{\text{PQ}})} + \frac{1}{\alpha_{14}(M_{\text{PQ}})}, \\ \frac{1}{\alpha_2(M_{\text{PQ}})} &= \frac{1}{\tilde{\alpha}_2(M_{\text{PQ}})} + \frac{1}{\alpha_{14}(M_{\text{PQ}})}, \\ \frac{1}{\alpha_3(M_{\text{PQ}})} &= \frac{1}{\tilde{\alpha}_3(M_{\text{PQ}})} + \frac{1}{\alpha_{14}(M_{\text{PQ}})}. \end{aligned} \quad (3.17)$$

Here $\tilde{\alpha}_{1,2,3}$ are the gauge couplings of $\text{SU}(3)_2 \times \text{SU}(2)_2 \times \text{U}(1)_2 (\subset \text{SU}(5)_2)$ and α_{14} is the gauge coupling of $\text{SU}(14)_1$. The beta functions at $M_{\text{PQ}} < \mu < M_{\text{GUT}}$ are given in eqs. (C.9, C.11). At the GUT scale M_{GUT} , the gauge symmetry is spontaneously broken by the VEV of Σ as

$$\text{SU}(5)_2 \rightarrow \text{SU}(3)_2 \times \text{SU}(2)_2 \times \text{U}(1)_2. \quad (3.18)$$

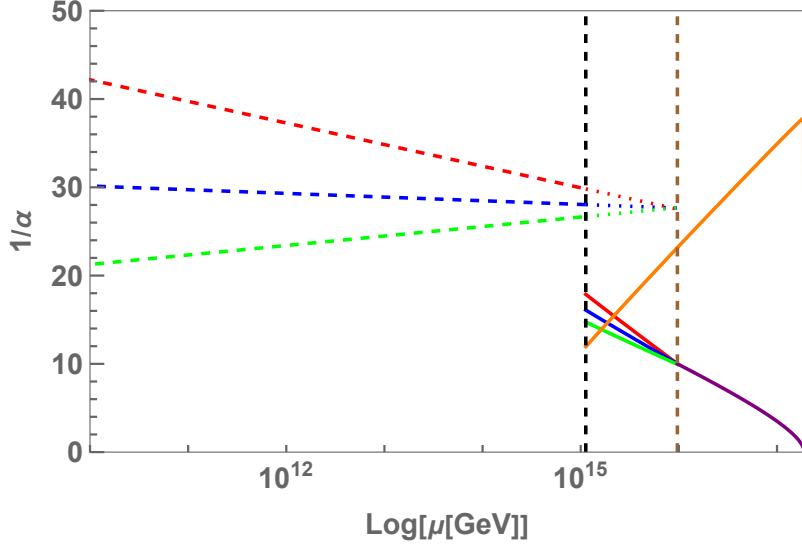


Figure 3. The running of gauge couplings with $M_{\text{PQ}} < M_{\text{GUT}}$, $\Lambda_{14} = 10^{14}$ GeV, and $(a, b, c) = (1, 2, 1)$. The red, blue, and green dashed lines show the SM gauge couplings, α_1 , α_2 , and α_3 , while the purple and orange solid lines denote α_5 and α_{14} , which are the gauge couplings of $\text{SU}(5)_2$ and $\text{SU}(14)_1$, respectively. The red, blue, and green solid lines denote $\tilde{\alpha}_1$, $\tilde{\alpha}_2$, and $\tilde{\alpha}_3$, which are the gauge couplings of $\text{U}(1)_2$, $\text{SU}(2)_2$, and $\text{SU}(3)_2$. The vertical black and brown dashed lines depict the PQ breaking and GUT scale, respectively. We set the MSSM particle mass as wino mass $M_{\tilde{W}} = 3$ TeV, the ratio of gluino and wino mass $M_{\tilde{g}}/M_{\tilde{W}} = 9$, the remaining sparticle mass $M_S = 100$ TeV, and $\tan \beta = 3$.

The tree level matching condition at $\mu = M_{\text{GUT}}$ is given as

$$\frac{1}{\tilde{\alpha}_a(M_{\text{GUT}})} = \frac{1}{\tilde{\alpha}_b(M_{\text{GUT}})} = \frac{1}{\alpha_5(M_{\text{GUT}})}, \quad (3.19)$$

where α_5 is the gauge coupling of $\text{SU}(5)_2$. The beta functions at $\mu > M_{\text{GUT}}$ are given in eqs. (C.12, C.14).

Figure 3 shows an example of successful GUT unification. We take the dynamical scale of $\text{SU}(14)_1$ gauge group as $\Lambda_{14} = 10^{14}$ GeV, and the PQ breaking and GUT scale for the case of $(a, b, c) = (1, 2, 1)$. At the PQ breaking scale, which is denoted by the vertical black dashed line, the gauge couplings for $\text{U}(1)$, $\text{SU}(2)$, and $\text{SU}(3)$ are changed to satisfy the matching conditions eq. (3.17). Above that scale, three gauge couplings are unified successfully at the GUT scale, which is depicted by the vertical brown dashed line. Thus, in the case of $M_{\text{GUT}} > M_{\text{PQ}}$, the value of unified coupling is greater than the case of $M_{\text{GUT}} < M_{\text{PQ}}$. This difference affects the proton lifetime discussed in the next subsection.

In figure 4, we show the scale Λ at which the Landau pole appears as a function of the axion decay constant f_a . The gray shaded region denotes below the Planck scale $M_P \simeq 2.4 \times 10^{18}$ GeV. In this analysis, we determine the PQ breaking and GUT scale by taking $(a, b, c) = (1, 2, 1)$ in the procedure discussed in section 3.1. We note that M_{PQ} and M_{GUT} can be determined by five choices of (a, b, c) in section 3.1 as well, however, the results are quite similar to the case of $(1, 2, 1)$. This figure shows that f_a should be higher

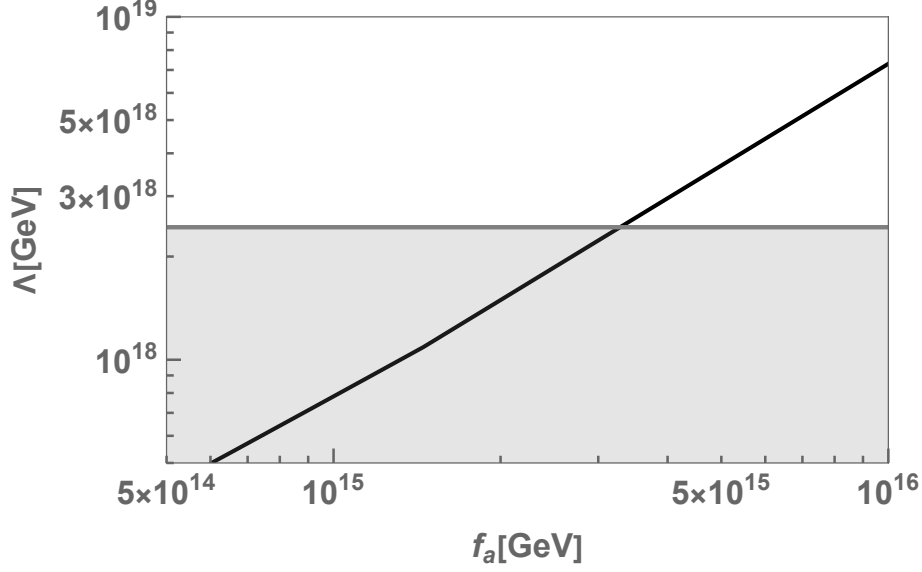


Figure 4. Black solid line shows the scale Λ for hitting the Landau pole as a function of the axion decay constant f_a in the case of $(a, b, c) = (1, 2, 1)$. The gray shaded region denotes below the plank scale $M_P \simeq 2.4 \times 10^{18}$ GeV.

than 3.4×10^{15} GeV to avoid the appearance of the Landau pole below the Planck scale. Our analysis is based on the minimal Higgs and GUT breaking sector; Σ , H , and \bar{H} . If we introduce additional Higgs multiplets, the Landau pole appears at lower scale and the constraint on f_a becomes stronger.

3.3 Proton decay

In this subsection, we discuss the proton lifetime in our model. In the minimal SUSY SU(5) GUT, the proton decay is induced by the exchange of the color-triplet Higgs and the heavy SU(5) gauge bosons, which is described by the dimension-five and -six effective operators, respectively. Since we assume $\mathcal{O}(100)$ TeV sfermion masses, the dimension-five proton decay operators are not constrained by the current observations [55, 56]. Thus, we discuss the dimension-six proton decay operators. In our analysis, we consider the $p \rightarrow \pi^0 e^+$ mode, which is constrained by the experiments most severely in the case of the dimension-six proton decay operators. In the fermion mass basis, these relevant interactions are expressed as [57–59]

$$\mathcal{L}_{\text{int}} = \frac{g_5}{\sqrt{2}} \left[-\bar{d}_{Ri}^c \gamma_\mu X_5^\mu L_i + e^{-i\varphi_i} \bar{Q}'_i \gamma_\mu X_5^\mu u_{Ri}^c + \bar{e}_{Ri}^c \gamma_\mu X_5^\mu (V_{\text{CKM}}^\dagger)_{ij} Q'_j + \text{h.c.} \right], \quad (3.20)$$

where $Q'_i \equiv (u_{Li}, (V_{\text{CKM}} d_L)_i)^T$, V_{CKM} is the Cabibbo-Kobayashi-Maskawa (CKM) matrix, g_5 is the SU(5) gauge coupling, X_5^μ is the SU(5) gauge bosons, and φ_i are the GUT phase factors [60].

In our current model, the SU(5) gauge bosons X_5^μ are mixed with the SU(14) gauge

bosons X_{14}^μ . The mass matrix of the gauge bosons is given as

$$M_X^2 = \begin{pmatrix} g_{14}^2 \phi^2 & -g_5 g_{14} \phi^2 \\ -g_5 g_{14} \phi^2 & 50g_5^2 \sigma^2 + g_5^2 \phi^2 \end{pmatrix}, \quad (3.21)$$

where g_{14} is the SU(14) gauge coupling. Let us denote the mass eigenvalues as M_1 and M_2 , and the mixing angle as θ . M_1 and M_2 are written as

$$M_{1,2}^2 = \frac{(g_5^2 + g_{14}^2) \phi^2 + 50g_5^2 \sigma^2 \pm \sqrt{[(g_5^2 + g_{14}^2) \phi^2 + 50g_5^2 \sigma^2]^2 - 200g_5^2 g_{14}^2 \phi^2 \sigma^2}}{2}, \quad (3.22)$$

and the mixing angle θ is determined from

$$\tan 2\theta = \frac{2g_5 g_{14} \phi^2}{50g_5^2 \sigma^2 + (g_5^2 - g_{14}^2) \phi^2}. \quad (3.23)$$

The mass eigenstates X_1^μ and X_2^μ are written in terms of the gauge eigenstates as

$$\begin{pmatrix} X_{14}^\mu \\ X_5^\mu \end{pmatrix} = \begin{pmatrix} \cos \theta & \sin \theta \\ -\sin \theta & \cos \theta \end{pmatrix} \begin{pmatrix} X_1^\mu \\ X_2^\mu \end{pmatrix}. \quad (3.24)$$

By integrating out both X_1^μ and X_2^μ , we can derive the dimension-six effective operators, and evolve their Wilson coefficients from M_{GUT} to the hadronic scale. As a result, the partial decay width for $p \rightarrow \pi^0 e^+$ mode is given by

$$\Gamma(p \rightarrow \pi^0 e^+) = \frac{m_p}{32\pi} \left(1 - \frac{m_\pi^2}{m_p^2}\right)^2 \left[|\mathcal{A}_L(p \rightarrow \pi^0 e^+)|^2 + |\mathcal{A}_R(p \rightarrow \pi^0 e^+)|^2 \right], \quad (3.25)$$

where $m_p = 0.938$ GeV and $m_\pi = 0.135$ GeV are the proton and pion mass [61]. The amplitudes \mathcal{A}_L and \mathcal{A}_R are

$$\begin{aligned} \mathcal{A}_L(p \rightarrow \pi^0 e^+) &= - \left[\frac{g_5^2 \sin^2 \theta}{M_1^2} + \frac{g_5^2 \cos^2 \theta}{M_2^2} \right] \cdot A_1 \cdot \langle \pi^0 | (ud)_{RuL} | p \rangle, \\ \mathcal{A}_R(p \rightarrow \pi^0 e^+) &= - \left[\frac{g_5^2 \sin^2 \theta}{M_1^2} + \frac{g_5^2 \cos^2 \theta}{M_2^2} \right] \cdot (1 + |V_{ud}|^2) \cdot A_2 \cdot \langle \pi^0 | (ud)_{RuL} | p \rangle, \end{aligned} \quad (3.26)$$

where V_{ud} is the (1,1) element of V_{CKM} [61]. The A_1 and A_2 are the renormalization factors [62, 63], and these depend on the hierarchy between M_{PQ} and M_{GUT} . For details of the calculation, see appendix D. For the case of $M_{\text{PQ}} > M_{\text{GUT}}$, A_1 and A_2 are the same as the usual SUSY SU(5) GUT case, and given by

$$\begin{aligned} A_1 &= A_L \cdot \left[\frac{\alpha_3(M_S)}{\alpha_3(M_{\text{GUT}})} \right]^{\frac{4}{9}} \left[\frac{\alpha_2(M_S)}{\alpha_2(M_{\text{GUT}})} \right]^{-\frac{3}{2}} \left[\frac{\alpha_1(M_S)}{\alpha_1(M_{\text{GUT}})} \right]^{-\frac{1}{18}} \\ &\quad \times \left[\frac{\alpha_3(M_Z)}{\alpha_3(M_S)} \right]^{\frac{2}{7}} \left[\frac{\alpha_2(M_Z)}{\alpha_2(M_S)} \right]^{\frac{27}{38}} \left[\frac{\alpha_1(M_Z)}{\alpha_1(M_S)} \right]^{-\frac{11}{82}}, \\ A_2 &= A_L \cdot \left[\frac{\alpha_3(M_S)}{\alpha_3(M_{\text{GUT}})} \right]^{\frac{4}{9}} \left[\frac{\alpha_2(M_S)}{\alpha_2(M_{\text{GUT}})} \right]^{-\frac{3}{2}} \left[\frac{\alpha_1(M_S)}{\alpha_1(M_{\text{GUT}})} \right]^{-\frac{23}{198}} \\ &\quad \times \left[\frac{\alpha_3(M_Z)}{\alpha_3(M_S)} \right]^{\frac{2}{7}} \left[\frac{\alpha_2(M_Z)}{\alpha_2(M_S)} \right]^{\frac{27}{38}} \left[\frac{\alpha_1(M_Z)}{\alpha_1(M_S)} \right]^{-\frac{23}{82}}, \end{aligned} \quad (3.27)$$

where $A_L \simeq 1.25$ is the long-distance QCD renormalization factor [64], and M_Z is Z boson scale. On the other hand, for the case of $M_{\text{PQ}} < M_{\text{GUT}}$, A_1 and A_2 are given by

$$\begin{aligned}
A_1 &= A_L \cdot \left[\frac{\tilde{\alpha}_3(M_{\text{PQ}})}{\tilde{\alpha}_3(M_{\text{GUT}})} \right]^{-\frac{4}{33}} \left[\frac{\tilde{\alpha}_2(M_{\text{PQ}})}{\tilde{\alpha}_2(M_{\text{GUT}})} \right]^{-\frac{1}{10}} \left[\frac{\tilde{\alpha}_1(M_{\text{PQ}})}{\tilde{\alpha}_1(M_{\text{GUT}})} \right]^{-\frac{11}{618}} \\
&\quad \times \left[\frac{\alpha_3(M_S)}{\alpha_3(M_{\text{PQ}})} \right]^{\frac{4}{9}} \left[\frac{\alpha_2(M_S)}{\alpha_2(M_{\text{PQ}})} \right]^{-\frac{3}{2}} \left[\frac{\alpha_1(M_S)}{\alpha_1(M_{\text{PQ}})} \right]^{-\frac{1}{18}} \\
&\quad \times \left[\frac{\alpha_3(M_Z)}{\alpha_3(M_S)} \right]^{\frac{2}{7}} \left[\frac{\alpha_2(M_Z)}{\alpha_2(M_S)} \right]^{\frac{27}{38}} \left[\frac{\alpha_1(M_Z)}{\alpha_1(M_S)} \right]^{-\frac{11}{82}}, \\
A_2 &= A_L \cdot \left[\frac{\tilde{\alpha}_3(M_{\text{PQ}})}{\tilde{\alpha}_3(M_{\text{GUT}})} \right]^{-\frac{4}{33}} \left[\frac{\tilde{\alpha}_2(M_{\text{PQ}})}{\tilde{\alpha}_2(M_{\text{GUT}})} \right]^{-\frac{1}{10}} \left[\frac{\tilde{\alpha}_1(M_{\text{PQ}})}{\tilde{\alpha}_1(M_{\text{GUT}})} \right]^{-\frac{23}{618}} \\
&\quad \times \left[\frac{\alpha_3(M_S)}{\alpha_3(M_{\text{PQ}})} \right]^{\frac{4}{9}} \left[\frac{\alpha_2(M_S)}{\alpha_2(M_{\text{PQ}})} \right]^{-\frac{3}{2}} \left[\frac{\alpha_1(M_S)}{\alpha_1(M_{\text{PQ}})} \right]^{-\frac{23}{198}} \\
&\quad \times \left[\frac{\alpha_3(M_Z)}{\alpha_3(M_S)} \right]^{\frac{2}{7}} \left[\frac{\alpha_2(M_Z)}{\alpha_2(M_S)} \right]^{\frac{27}{38}} \left[\frac{\alpha_1(M_Z)}{\alpha_1(M_S)} \right]^{-\frac{23}{82}}.
\end{aligned} \tag{3.28}$$

The $\langle \pi^0 | (ud)_{RuL} | p \rangle$ is the hadronic matrix element computed in lattice QCD calculations and the numerical value is [65]

$$\langle \pi^0 | (ud)_{RuL} | p \rangle = -0.131(4)(13) \text{ GeV}^2. \tag{3.29}$$

In figure 5, we show the renormalization factors A_1 and A_2 in eqs. (3.27, 3.28) as a function of the axion decay constant f_a . Here we estimate the GUT scale as $\alpha_a(M_{\text{GUT}}) = \alpha_b(M_{\text{GUT}})$ for $(a, b) = (1, 2), (2, 3), (3, 1)$, and take c to be higher PQ breaking scale in the choice of (a, b) . Then, the red, blue, and green curves in figure 5 indicate the results for $(a, b, c) = (1, 2, 2), (2, 3, 3)$, and $(3, 1, 3)$, respectively. In the case of $M_{\text{PQ}} > M_{\text{GUT}}$, the renormalization factors A_1 and A_2 are independent of f_a . On the other hand, in the case of $M_{\text{PQ}} < M_{\text{GUT}}$, the value of the gauge coupling at the GUT scale becomes larger for lower f_a . Then, the renormalization factors A_1 and A_2 also become larger for lower f_a . Note that the behavior of A_1 and A_2 also connects smoothly including in the case of $M_{\text{PQ}} \simeq M_{\text{GUT}}$.

Figure 6 shows the proton lifetime τ_p as a function of the axion decay constant f_a . As the same as in figure 5, we set the PQ breaking and GUT scale from $(a, b, c) = (1, 2, 2), (2, 3, 3)$, and $(3, 1, 3)$, and red, blue, and green solid curves indicate these results, respectively. The difference among the choices of (a, b, c) should be understood as the uncertainty from the threshold correction at the PQ breaking and GUT scale. The difference between those three curves should roughly correspond to the uncertainty from the threshold correction of the PQ breaking and GUT scale particles, and this affects the proton lifetime estimation.

Let us discuss f_a dependence of the proton lifetime shown in figure 6. If M_{PQ} is lower than M_{GUT} , the gauge coupling relevant to proton decay becomes larger than the minimal SU(5) GUT as indicated in figure 3. Then, the proton lifetime becomes shorter and this effect is more significant for lower f_a . If the axion decay constant f_a is very low, the Landau pole of the gauge coupling appears below $\sim 10^{16}$ GeV and the picture of

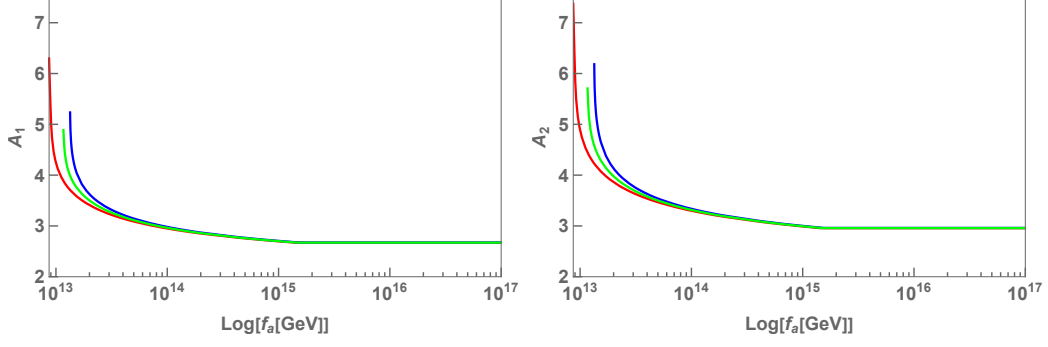


Figure 5. These plots show the renormalization factors A_1 (A_2) in eqs. (3.27, 3.28) as a function of the axion decay constant f_a in left (right) panel. Red, blue, and green solid curves indicate the results for $(a, b, c) = (1, 2, 2)$, $(2, 3, 3)$, and $(3, 1, 3)$, respectively.

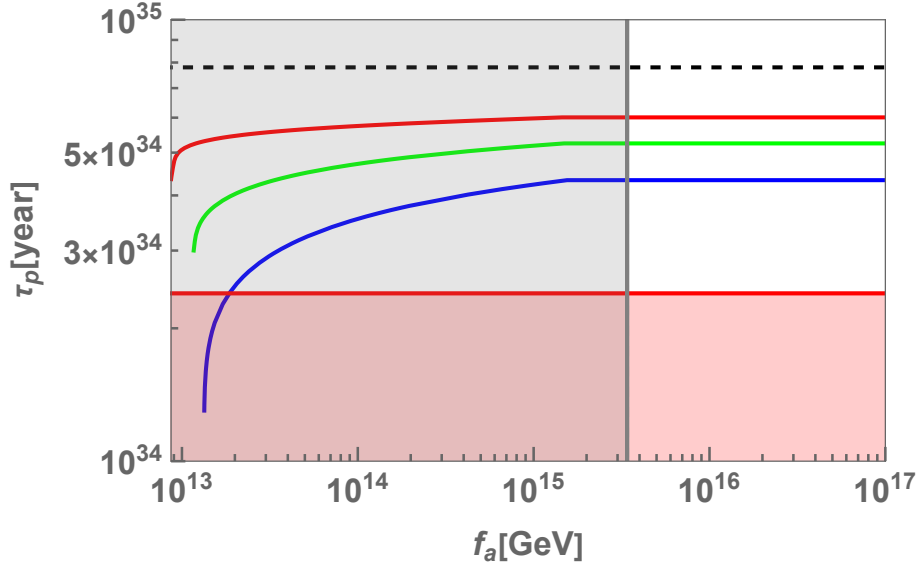


Figure 6. This plot shows proton lifetime τ_p as a function of the axion decay constant f_a . Red, blue, and green solid curves indicate the results for $(a, b, c) = (1, 2, 2)$, $(2, 3, 3)$, and $(3, 1, 3)$, respectively. The excluded region for proton lifetime by Super-Kamiokande experiment is the red shaded region as $\tau_p(p \rightarrow \pi^0 e^+) > 2.4 \times 10^{34}$ years [66] and the black dashed line depicts the future sensitivity by the Hyper-Kamiokande experiment, $\tau_p(p \rightarrow \pi^0 e^+) = 7.8 \times 10^{34}$ years [67]. Also, the gray shaded region denotes the constraint by the Landau pole.

coupling unification is destroyed. From this constraint, we find that the lower bound of f_a is 8.7×10^{12} GeV for $(a, b, c) = (1, 2, 2)$, while in the other two choices, this is 1.3×10^{13} GeV for $(a, b, c) = (2, 3, 3)$, and 1.2×10^{13} GeV for $(a, b, c) = (3, 1, 3)$, respectively. In figure 6, we plot each result from its lower bound of f_a , and thus the results for $(a, b, c) = (2, 3, 3)$ and $(3, 1, 3)$ are not drawn below each lower bound. In addition, the lower bound of the proton lifetime is different between the three choices, and the proton lifetime is longer than 1.3×10^{34} years, which corresponds to the results with the lower bound of f_a for $(a, b, c) = (2, 3, 3)$. Note that, as we have seen in section 3.2 and figure 4, in the case of

$M_{\text{GUT}} > M_{\text{PQ}}$, the Landau pole of the gauge coupling appears below M_P . On the other hand, if M_{PQ} is higher than M_{GUT} , the gauge coupling relevant to the proton decay is similar to the minimal SU(5) GUT as indicated in figure 2. Thus, the proton lifetime is almost independent of f_a as shown in figure 6. The current constraint on the proton lifetime of this mode is $\tau_p(p \rightarrow \pi^0 e^+) > 2.4 \times 10^{34}$ years [66], and the future sensitivity at the Hyper-Kamiokande experiment is $\tau_p(p \rightarrow \pi^0 e^+) = 7.8 \times 10^{34}$ years [67]. Therefore, regardless of the value of f_a , our model can be tested by future proton decay searches.

Finally, we briefly comment on the behavior of three curves in figure 6. Both the GUT breaking VEV σ and renormalization factors A_1 and A_2 become larger for lower f_a , and the case of $(a, b, c) = (1, 2, 2)$ is more significant than the other two cases as shown in figures 1 and 5. As a result, by combining the effect of the renormalization factors with the GUT breaking VEV, the proton lifetime becomes shorter for lower f_a because of large enhancement in A_1 and A_2 .

3.4 Small instanton

Let us comment on small instanton contributions to the axion mass [68–72]. SU(5)₂ gauge interaction is asymptotic non-free in the energy scale above the PQ breaking scale. Thus, we could expect that the small instanton affects the QCD axion mass. However, this contribution is extremely small as we explain below.

SU(5)₂ instanton provides a 't Hooft vertex with 10 SU(5)₂ gauginos, 14 \bar{F}_q fermions, 14 $\bar{F}_{\bar{q}}$ fermions, and MSSM fermions as external legs. Let us discuss the contraction of fermion lines of SU(5)₂ gauginos, \bar{F}_q , and $\bar{F}_{\bar{q}}$. Total R-charge of these legs is -18 . To have a contribution to the axion mass, we have to make contractions of fermion lines and the remaining external legs should be only PQ-charged scalar field with VEV. Since the scalar fields of \bar{F}_q and $\bar{F}_{\bar{q}}$ do not have R-charge, we need to consume 9 insertions of gaugino mass m_λ to have only scalar field as external log by contracting fermion lines. Thus, the axion mass squared suffers from quite strong suppression factor $(m_\lambda/\Lambda)^9 \sim 10^{-105} (m_\lambda/1 \text{ TeV})^9 (\Lambda/M_{\text{pl}})^{-9}$. Also, the additional suppression factor should come from contraction of MSSM fermions, e.g., $K \equiv \prod_q (y_q/4\pi) \sim 10^{-23}$ [73]. Thus, we conclude that the small instanton contribution to the axion mass is negligibly small in the current model.

3.5 Cosmology

The QCD axion and its superpartners play some important roles in cosmology and it highly depends on the details of scenario. Here we briefly mention the cosmological aspects of the present model.

In the present model, the number of vacua is $N_{\text{DW}} = 24$ and potentially we suffer from domain-wall problem. Also, there exists U(1)_d global symmetry and the lightest particle with nonzero U(1)_d charge has a mass of the order of M_{PQ} . Since those stable domain-wall network and particles can overclose the universe, we assume the inflation energy scale H_{inf} is sufficiently low such that PQ symmetry had already broken during inflation.

The QCD axion is a good candidate of the dark matter. As we have discussed, the decay constant of the axion in the current model is above $\sim 10^{13}$ GeV which is higher than the canonical value of $f_a \sim 10^{12}$ GeV for the misalignment scenario. See, e.g., Ref. [74]. Thus,

we need to assume that the initial misalignment angle is suppressed by some mechanism or entropy production between the onset of the axion coherent oscillation and Big Bang nucleosynthesis diluted the energy density of the axion [75–77].

If our universe has experienced a first order phase transition, gravitational waves (GW) from the phase transition can be produced. From this point of view, the confinement phase transition of Sp(4) SUSY pure Yang-Mills theory is interesting. Eq. (3.2) indicates that the confinement scale of Sp(4) gauge theory is below the PQ breaking scale, and this phase transition can happen after the end of inflation. The lattice simulation indicates the order of confinement phase transition is the first order in Sp(4) pure Yang-Mills theory [78, 79] and QCD with adjoint fermion [80], though a lattice simulation of Sp(4) SUSY pure Yang-Mills theory is not available. The sound wave after bubble collision is considered to be the main source of GW and its peak frequency and amplitude of the GW signal from phase transitions are estimated as [81–83]

$$f_{\text{peak}} \sim 1.9 \times 10^8 \text{ Hz} \times \left(\frac{\tilde{\beta}}{10^5} \right) \left(\frac{1}{v_w} \right) \left(\frac{T}{10^{10} \text{ GeV}} \right) \left(\frac{g_*}{100} \right)^{1/6}, \quad (3.30)$$

$$\Omega_{\text{GW,peak}} h^2 \sim 2.65 \times 10^{-16} \times \left(\frac{\tilde{\beta}}{10^5} \right)^{-1} \left(\frac{\kappa^2}{10^{-5}} \right) \left(\frac{\alpha}{1+\alpha} \right)^2 \left(\frac{g_*}{100} \right)^{-1/3} \left(\frac{g_{*,\text{dark}}}{g_{*,\text{dark}} + g_{*,\text{SM}}} \right)^2, \quad (3.31)$$

where α is (dimensionless) latent heat α , $\tilde{\beta}$ is (dimensionless) inverse time of duration of the phase transition, and v_w is the bubble wall velocity. Ref. [84] shows the typical size of $\tilde{\beta}$ is 10^4 – 10^5 , which indicates $f_{\text{peak}} \sim \mathcal{O}(10^8) \text{ Hz} \times (\Lambda_{\text{Sp}(4)}/10^{10} \text{ GeV})$. Although it is quite challenging to probe such GW with high frequency, there exist several proposals to probe such a frequency range [85].

4 Conclusions and discussions

In this paper, we have discussed axion models based on supersymmetric chiral gauge theories; SUSY Georgi-Glashow type model and SUSY Bars-Yankielowicz type model. Thanks to small SUSY soft breaking, we can apply the analysis presented in Refs. [23, 24] and we found that, in both models, spontaneous breaking of PQ symmetry is induced by non-perturbative dynamics. We have also discussed a GUT-motivated QCD axion model. We have shown that the proton lifetime becomes shorter for smaller f_a and our model can be tested by future proton decay searches. Also, a high scale f_a is preferred to avoid the Landau pole of the gauge coupling below the Planck scale. Its cosmological aspects have been discussed, and the gravitational wave from the confinement phase transition of the unbroken Sp(4) gauge sector would be an interesting target for future experiments.

In the closing of this paper, we briefly mention non-supersymmetric limit of the current model in which all of sfermions and gauginos are decoupled. This limit is interesting because gauge invariant PQ charged scalar operator consists of at least six fermion fields and it has at least dimension 9. Thus, the PQ symmetry arises as an accidental symmetry and the axion quality problem can be relaxed. However, in such a regime, supersymmetry is badly

	SU(2N)	SU(2N - 4)	U(1) _A	U(1)	U(1) _R
\bar{F}	\square	\square	1	$2N - 2$	$1 - \frac{2N}{N-2}$
A	\square	1	0	$-2N + 4$	1
$\Lambda^{b_{\text{SU}(2N)}}$	1	1	$2N - 4$	$2N$	0
PfA	1	1	0	$N(-2N + 4)$	N
PfX	1	1	$2N - 4$	$N(2N - 4)$	$-N - 6$

Table 6. The matter content in SUSY Georgi-Glashow model.

broken and it is quite difficult to study in the current method. See, e.g., a discussion in section 2.4 of Ref. [86]. There has been literature which discuss such a model by using the most attractive channel (MAC) analysis [87, 88] and it predicts a different IR picture; 't Hooft anomaly matching condition is satisfied by not axion but massless baryon (see, e.g., [89]). To have definite conclusions in this limit, we would need a non-perturbative analysis such as lattice gauge theory simulations.

Note added: As this paper was being completed we became aware of overlapping work in preparation from another group [90].

Acknowledgements

RS thanks Pablo Quílez for useful discussions. The work of RS is supported in part by JSPS KAKENHI Grant Numbers 23K03415, 24H02236, and 24H02244. The work of ST is supported by JST SPRING, Grant Number JPMJSP2132.

A Dynamical superpotential in SUSY Georgi-Glashow type model

In this appendix, we discuss the dynamical superpotential in SU(2N) chiral gauge theory discussed in Ref. [33, 34]. As far as we know, the explicit coefficient of the dynamical superpotential has not given in the literature though it can be calculated in the same way as the coefficient of ADS superpotential [91].

We introduce $2N - 4$ flavors of anti-fundamental chiral multiplets \bar{F} (\square) and an anti-symmetric tensor chiral multiplet A (\square). Then, we can define the following gauge-invariant flavor singlet chiral fields:

$$\text{Pf}A \equiv \frac{1}{2^N N!} \epsilon^{i_1 \cdots i_{2N}} A_{i_1 i_2} \cdots A_{i_{2N-1} i_{2N}}, \quad (\text{A.1})$$

$$\text{Pf}X \equiv \frac{1}{2^{N-2} (N-2)!} \epsilon^{a_1 \cdots a_{2N-4}} X_{a_1 a_2} \cdots X_{a_{2N-5} a_{2N-4}}. \quad (\text{A.2})$$

where $X_{ab} \equiv A_{ij} \bar{F}_a^i \bar{F}_b^j$. Note that a and b are flavor indices and they run from 1 to $2N - 4$, and i and j are gauge indices and they run from 1 to $2N$. These fields have global symmetries and their charges are summarized in Tab. 6. By using $U(1) \times U(1)_R$ symmetry and a spurious $U(1)_A$ symmetry, we can write the dynamical superpotential at low energy

as

$$W = c \left(\frac{\Lambda_{\text{SU}(2N)}^{b_{\text{SU}(2N)}}}{(\text{Pf}A)(\text{Pf}X)} \right)^{1/3}, \quad (\text{A.3})$$

where $b_{\text{SU}(2N)}$ is the one-loop beta function coefficient given as

$$b_{\text{SU}(2N)} = 3 \times 2N - \underbrace{(2N-4) \times \frac{1}{2}}_{\bar{F}} - \underbrace{\frac{1}{2}(2N-2)}_A = 4N+3. \quad (\text{A.4})$$

c is a constant which we determine in the following of this appendix.

By assuming $\text{Pf}A \neq 0$ and $\text{Pf}X \neq 0$, the superpotential eq. (A.3) can be understood as a result of gaugino condensation of unbroken gauge symmetry. For simplicity of the analysis, we assume the VEV of A and \bar{F} as

$$\langle A \rangle = v_A (i\sigma^2 \otimes I_N), \quad \langle \bar{F} \rangle = v_{\bar{F}} \begin{pmatrix} I_{N-4} \\ 0 \end{pmatrix}, \quad (\text{A.5})$$

with $v_{\bar{F}} \ll v_A$. Note that A and \bar{F} are canonically normalized as $K = A_{ij}A^{*ij} + \bar{F}_a^i \bar{F}_i^{*a}$ with $A_{ij} = -A_{ji}$. Because of the hierarchy $v_{\bar{F}} \ll v_A$, we can understand the spontaneous breaking of gauge symmetry as two steps. First, $\langle A \rangle$ breaks $\text{SU}(2N)$ gauge symmetry into $\text{Sp}(2N)$. Then, at lower energy scale, $\langle \bar{F} \rangle$ breaks $\text{Sp}(2N)$ gauge symmetry into $\text{Sp}(4)$.

Below the energy scale of v_A (but still above $v_{\bar{F}}$), the low energy effective theory is described by $\text{Sp}(2N)$ gauge theory. Let us discuss the matching condition between $\Lambda_{\text{SU}(2N)}$ and $\Lambda_{\text{Sp}(2N)}$. $\text{SU}(2N)$ gauge theory has $4N^2 - 1$ gauge bosons and $\text{Sp}(2N)$ gauge theory has $2N^2 + N$ gauge bosons. A has $2N^2 - N$ degrees of freedom in total. Among them, $2N^2 - N - 1$ degrees of freedom in A are eaten by the massive gauge bosons, and the remaining one degree of freedom in A parametrize the direction of v_A . \bar{F} behaves as fundamental representation under $\text{Sp}(2N)$ gauge symmetry. The massive gauge bosons form \square of $\text{Sp}(2N)$ and their mass is $m_W = 2gv_A$. The matching condition between two holomorphic couplings is

$$\left(\frac{\Lambda_{\text{SU}(2N)}}{2v_A} \right)^{b_{\text{SU}(2N)}} = \left(\frac{\Lambda_{\text{Sp}(2N)}}{2v_A} \right)^{b_{\text{Sp}(2N)}}. \quad (\text{A.6})$$

See e.g. [92, 93] and footnote 13 in [94]. The coefficient $b_{\text{Sp}(2N)}$ in one-loop beta function is given as

$$b_{\text{Sp}(2N)} = \frac{3}{2}(2N+2) - \underbrace{(2N-4) \times \frac{1}{2}}_{\bar{F}} = 2N+5. \quad (\text{A.7})$$

Then, we obtain the matching condition:

$$\Lambda_{\text{Sp}(2N)}^{2N+5} = \frac{\Lambda_{\text{SU}(2N)}^{4N+3}}{(2v_A)^{2N-2}}. \quad (\text{A.8})$$

Below the energy scale of $v_{\bar{F}}$, the low energy effective theory is described by $\text{Sp}(4)$ gauge theory. Let us discuss the matching condition between $\Lambda_{\text{Sp}(2N)}$ and $\Lambda_{\text{Sp}(4)}$. $\text{Sp}(2N)$ gauge theory has $2N^2 + N$ gauge bosons and $\text{Sp}(4)$ gauge theory has 10 gauge bosons. \bar{F} has $4N^2 - 8N$ degrees of freedom in total. Among them, $2N^2 + N - 10$ degrees of freedom are eaten by the massive gauge bosons, and $2N^2 - 9N + 9$ are NG bosons in $\text{SU}(2N - 4)/\text{Sp}(2N - 4)$, and the remaining one parameterizes in the direction of $v_{\bar{F}}$. Massive gauge boson form $(2N - 4) \times \square + (2N^2 - 7N + 6) \times \mathbf{1}$ of $\text{Sp}(4)$, and the mass of \square massive gauge boson is $gv_{\bar{F}}/\sqrt{2}$. The coefficient $b_{\text{Sp}(4)}$ in one-loop beta function is given as

$$b_{\text{Sp}(4)} = \frac{3}{2} \times 6 = 9. \quad (\text{A.9})$$

The matching condition between two holomorphic couplings is

$$\left(\frac{\Lambda_{\text{SU}(2N)}}{v_{\bar{F}}/\sqrt{2}} \right)^{b_{\text{SU}(2N)}} = \left(\frac{\Lambda_{\text{Sp}(4)}}{v_{\bar{F}}/\sqrt{2}} \right)^{b_{\text{Sp}(4)}}. \quad (\text{A.10})$$

Thus, we obtain the matching condition:

$$\Lambda_{\text{Sp}(4)}^9 = \frac{\Lambda_{\text{Sp}(2N)}^{2N+5}}{(v_{\bar{F}}/\sqrt{2})^{2N-4}}. \quad (\text{A.11})$$

This matching condition is consistent with the condition given in [95]. To summarize, in the limit of $v_{\bar{F}} \ll v_A$, we obtain

$$\Lambda_{\text{Sp}(4)}^9 = 2^{-N} \frac{\Lambda_{\text{SU}(2N)}^{4N+3}}{v_{\bar{F}}^{2N-4} v_A^{2N-2}}. \quad (\text{A.12})$$

Note that $\text{Pf}A = v_A^N$, $\text{Pf}X = v_A^{N-2} v_{\bar{F}}^{2N-4}$. The generic matching condition between $\Lambda_{\text{SU}(2N)}$ and $\Lambda_{\text{Sp}(4)}$ is

$$\Lambda_{\text{Sp}(4)}^9 = 2^{-N} \frac{\Lambda_{\text{SU}(2N)}^{4N+3}}{(\text{Pf}A)(\text{Pf}X)}. \quad (\text{A.13})$$

For $\text{Sp}(2N)$ pure SUSY Yang-Mills theory, its gaugino condensation induces the effective superpotential as $W = (N + 1)2^{(N-1)/(N+1)} \Lambda_{\text{Sp}(2N)}^3$ [95, 96]. Thus, we obtain

$$W = 3 \cdot 2^{(1-N)/3} \left(\frac{\Lambda_{\text{SU}(2N)}^{4N+3}}{(\text{Pf}A)(\text{Pf}X)} \right)^{1/3}. \quad (\text{A.14})$$

We can see the dynamical superpotential given in eq. (2.12) is equivalent to the above superpotential.

B The GUT breaking VEV σ

In this appendix, we calculate the GUT breaking VEV σ in the setup discussed in section 3 from M_{PQ} , M_{GUT} , and ϕ . For this discussion, we utilize the holomorphic gauge coupling

g_h , which is related to the canonical gauge coupling g_c as [97–100],

$$\frac{1}{g_h^2(\mu)} = \frac{1}{g_c^2(\mu)} + \frac{2C(G)}{8\pi^2} \log g_c(\mu) + \sum_i \frac{S(R_i)}{8\pi^2} \log Z_i(\mu), \quad (\text{B.1})$$

where $S(R_i)$ is the Dynkin index of representation R_i , $C(R_i)$ is the Casimir invariant, Z_i is the wave function renormalization factor for chiral multiplet i , and μ is the renormalization scale. Because of holomorphy, the running of the holomorphic coupling is one-loop exact. Also, the matching condition of the holomorphic coupling is satisfied at the VEV of symmetry breaking as we will see below.

Let us discuss the matching condition of the gauge coupling between UV and IR Lagrangian in a simplified model. We consider SU(5) gauge theory and introduce an adjoint Higgs chiral multiplet Σ . We assume that the SU(5) gauge symmetry is broken into SU(3) \times SU(2) \times U(1) gauge symmetry by the VEV $\langle \Sigma \rangle = \sigma \text{diag}(2, 2, 2, -3, -3)$. The canonical gauge coupling in $\overline{\text{DR}}$ scheme is satisfied with the following matching condition [92];

$$g_{1,c}(M_V) = g_{2,c}(M_V) = g_{3,c}(M_V) = g_{5,c}(M_V), \quad (\text{B.2})$$

where $g_{a,c}$ ($a = 1, 2, 3, 5$) are the canonical gauge couplings of U(1), SU(2), SU(3), and SU(5) gauge group, and M_V is the mass of massive SU(5) gauge bosons. The holomorphic gauge coupling $g_{a,h}(\mu)$ can be related to the canonical gauge coupling $g_{a,c}(M_V)$ by using eq. (B.1) as

$$\frac{8\pi^2}{g_{5,h}^2(\mu)} = \frac{8\pi^2}{g_{5,c}^2(M_V)} + b_5 \log \left(\frac{\mu}{M_V} g_{5,c}^{10/b_5}(M_V) Z_\Sigma^{5/b_5}(M_V) \right), \quad (\text{B.3})$$

$$\frac{8\pi^2}{g_{3,h}^2(\mu)} = \frac{8\pi^2}{g_{3,c}^2(M_V)} + b_3 \log \left(\frac{\mu}{M_V} g_{3,c}^{6/b_3}(M_V) Z_\Sigma^{3/b_3}(M_V) \right), \quad (\text{B.4})$$

$$\frac{8\pi^2}{g_{2,h}^2(\mu)} = \frac{8\pi^2}{g_{2,c}^2(M_V)} + b_2 \log \left(\frac{\mu}{M_V} g_{2,c}^{4/b_2}(M_V) Z_\Sigma^{2/b_2}(M_V) \right), \quad (\text{B.5})$$

$$\frac{8\pi^2}{g_{1,h}^2(\mu)} = \frac{8\pi^2}{g_{1,c}^2(M_V)} + b_1 \log \left(\frac{\mu}{M_V} \right), \quad (\text{B.6})$$

where $g_{a,h}$ ($a = 1, 2, 3, 5$) are the holomorphic gauge couplings of U(1), SU(2), SU(3), and SU(5) gauge group, $b_a = (0, 4, 6, 10)$ ($a = 1, 2, 3, 5$) are the one-loop beta coefficients, and Z_Σ is the wave function renormalization factor of Σ . Since the mass of SU(5) gauge boson can be written as $M_V = 5\sqrt{2}\sqrt{Z_\Sigma}g_{5,c}\sigma$ [93], eqs. (B.2)–(B.6) tell us that

$$g_{1,h}(5\sqrt{2}\sigma) = g_{2,h}(5\sqrt{2}\sigma) = g_{3,h}(5\sqrt{2}\sigma) = g_{5,h}(5\sqrt{2}\sigma). \quad (\text{B.7})$$

This matching condition is also satisfied in the case of SU(5) GUT because the MSSM chiral multiplets are completely included in the SU(5) multiplets. Therefore, we can derive the GUT breaking VEV by using the matching condition of each holomorphic coupling for U(1), SU(2), and SU(3) given in eq. (B.7). In our model, the GUT breaking VEV depends on the hierarchy between M_{PQ} and M_{GUT} . In both cases, we take each holomorphic coupling

at SUSY breaking scale $M_S = 100$ TeV as the initial parameters. This can be obtained by the values of the canonical gauge couplings, and we evaluate the running of the canonical gauge couplings at two-loop level and the Yukawa coupling at one-loop level as the same as discussion in section 3.2.

B.1 The case of $M_{PQ} > M_{GUT}$

The holomorphic gauge coupling at $\mu = M_S$ is calculated from eq. (B.1) with $\mu = M_S$. Here we canonically normalize the chiral multiplets at $\mu = M_{GUT}$, i.e., we take $Z(M_{GUT}) = 1$. Then, we can calculate $Z_i(M_S)$ for chiral multiplet i as

$$Z_i(M_S) = \exp \left(\int_{M_S}^{M_{GUT}} \gamma_i d \log \mu \right). \quad (B.8)$$

The anomalous dimension γ_i for each MSSM chiral multiplet i is given by (e.g. Ref. [101]),

$$\gamma_{Q_{1,2}} = \frac{1}{16\pi^2} \left[-\frac{16}{3}g_3^2 - 3g_2^2 - \frac{1}{15}g_1^2 \right], \quad (B.9)$$

$$\gamma_{Q_3} = \frac{1}{16\pi^2} \left[2y_t^2 - \frac{16}{3}g_3^2 - 3g_2^2 - \frac{1}{15}g_1^2 \right], \quad (B.10)$$

$$\gamma_{\bar{U}_{1,2}} = \frac{1}{16\pi^2} \left[-\frac{16}{3}g_3^2 - \frac{16}{15}g_1^2 \right], \quad (B.11)$$

$$\gamma_{\bar{U}_3} = \frac{1}{16\pi^2} \left[4y_t^2 - \frac{16}{3}g_3^2 - \frac{16}{15}g_1^2 \right], \quad (B.12)$$

$$\gamma_{\bar{D}_i} = \frac{1}{16\pi^2} \left[-\frac{16}{3}g_3^2 - \frac{4}{15}g_1^2 \right], \quad (B.13)$$

$$\gamma_{L_i} = \frac{1}{16\pi^2} \left[-3g_2^2 - \frac{3}{5}g_1^2 \right], \quad (B.14)$$

$$\gamma_{\bar{E}_i} = \frac{1}{16\pi^2} \left[-\frac{12}{5}g_1^2 \right], \quad (B.15)$$

$$\gamma_{H_u} = \frac{1}{16\pi^2} \left[6y_t^2 - 3g_2^2 - \frac{3}{5}g_1^2 \right], \quad (B.16)$$

$$\gamma_{H_d} = \frac{1}{16\pi^2} \left[-3g_2^2 - \frac{3}{5}g_1^2 \right]. \quad (B.17)$$

Here, we introduce the top Yukawa coupling as $W = y_t Q_3 \bar{U}_3 H_u$. Then, at one-loop level, the wave function renormalization factor for each MSSM chiral multiplet is given as

$$Z_{Q_{1,2}}(M_S) = \left[\frac{g_{1,c}(M_{GUT})}{g_{1,c}(M_S)} \right]^{-1/99} \left[\frac{g_{2,c}(M_{GUT})}{g_{2,c}(M_S)} \right]^{-3} \left[\frac{g_{3,c}(M_{GUT})}{g_{3,c}(M_S)} \right]^{16/9}, \quad (B.18)$$

$$Z_{Q_3}(M_S) = \left[\frac{y_t(M_{GUT})}{y_t(M_S)} \right]^{1/3} \left[\frac{g_{1,c}(M_{GUT})}{g_{1,c}(M_S)} \right]^{10/297} \left[\frac{g_{2,c}(M_{GUT})}{g_{2,c}(M_S)} \right]^{-2} \left[\frac{g_{3,c}(M_{GUT})}{g_{3,c}(M_S)} \right]^{32/27}, \quad (B.19)$$

$$Z_{\bar{U}_{1,2}}(M_S) = \left[\frac{g_{1,c}(M_{GUT})}{g_{1,c}(M_S)} \right]^{-16/99} \left[\frac{g_{3,c}(M_{GUT})}{g_{3,c}(M_S)} \right]^{16/9}, \quad (B.20)$$

$$Z_{\bar{U}_3}(M_S) = \left[\frac{y_t(M_{\text{GUT}})}{y_t(M_S)} \right]^{2/3} \left[\frac{g_{1,c}(M_{\text{GUT}})}{g_{1,c}(M_S)} \right]^{-2/27} \left[\frac{g_{2,c}(M_{\text{GUT}})}{g_{2,c}(M_S)} \right]^2 \left[\frac{g_{3,c}(M_{\text{GUT}})}{g_{3,c}(M_S)} \right]^{16/27}, \quad (\text{B.21})$$

$$Z_{\bar{D}_i}(M_S) = \left[\frac{g_{1,c}(M_{\text{GUT}})}{g_{1,c}(M_S)} \right]^{-4/99} \left[\frac{g_{3,c}(M_{\text{GUT}})}{g_{3,c}(M_S)} \right]^{16/9}, \quad (\text{B.22})$$

$$Z_{L_i}(M_S) = \left[\frac{g_{1,c}(M_{\text{GUT}})}{g_{1,c}(M_S)} \right]^{-1/11} \left[\frac{g_{2,c}(M_{\text{GUT}})}{g_{2,c}(M_S)} \right]^{-3}, \quad (\text{B.23})$$

$$Z_{\bar{E}_i}(M_S) = \left[\frac{g_{1,c}(M_{\text{GUT}})}{g_{1,c}(M_S)} \right]^{-4/11}, \quad (\text{B.24})$$

$$Z_{H_u}(M_S) = \left[\frac{y_t(M_{\text{GUT}})}{y_t(M_S)} \right] \left[\frac{g_{1,c}(M_{\text{GUT}})}{g_{1,c}(M_S)} \right]^{4/99} \left[\frac{g_{3,c}(M_{\text{GUT}})}{g_{3,c}(M_S)} \right]^{-16/9}, \quad (\text{B.25})$$

$$Z_{H_d}(M_S) = \left[\frac{g_{1,c}(M_{\text{GUT}})}{g_{1,c}(M_S)} \right]^{-1/11} \left[\frac{g_{2,c}(M_{\text{GUT}})}{g_{2,c}(M_S)} \right]^{-3}, \quad (\text{B.26})$$

where $g_{a,c}$ ($a = 1-3$) are the canonical gauge couplings for $U(1)_Y$, $SU(2)_L$, and $SU(3)_c$. The holomorphic couplings for $SU(3)_c$, $SU(2)_L$, and $U(1)_Y$ at M_S are given by

$$\begin{aligned} \frac{1}{g_{3,h}^2(M_S)} = & \frac{1}{g_{3,c}^2(M_S)} + \frac{3 \log g_{3,c}(M_S)}{4\pi^2} + \frac{1}{16\pi^2} \left[4 \log Z_{Q_{1,2}}(M_S) + 2 \log Z_{Q_3}(M_S) \right. \\ & \left. + 2 \log Z_{\bar{U}_{1,2}}(M_S) + \log Z_{\bar{U}_3}(M_S) + 3 \log Z_{\bar{D}}(M_S) \right], \end{aligned} \quad (\text{B.27})$$

$$\begin{aligned} \frac{1}{g_{2,h}^2(M_S)} = & \frac{1}{g_{2,c}^2(M_S)} + \frac{\log g_{2,c}(M_S)}{2\pi^2} + \frac{1}{16\pi^2} \left[6 \log Z_{Q_{1,2}}(M_S) + 3 \log Z_{Q_3}(M_S) \right. \\ & \left. + 3 \log Z_L(M_S) + \log Z_{H_u}(M_S) + \log Z_{H_d}(M_S) \right], \end{aligned} \quad (\text{B.28})$$

$$\begin{aligned} \frac{1}{g_{1,h}^2(M_S)} = & \frac{1}{g_{1,c}^2(M_S)} + \frac{3}{40\pi^2} \left[\frac{1}{3} \log Z_{Q_{1,2}}(M_S) + \frac{1}{6} \log Z_{Q_3}(M_S) + \frac{8}{3} \log Z_{\bar{U}_{1,2}}(M_S) \right. \\ & + \frac{4}{3} \log Z_{\bar{U}_3}(M_S) + \log Z_{\bar{D}}(M_S) + \frac{3}{2} \log Z_L(M_S) \\ & \left. + 3 \log Z_{\bar{E}}(M_S) + \frac{1}{2} \log Z_{H_u}(M_S) + \frac{1}{2} \log Z_{H_d}(M_S) \right], \end{aligned} \quad (\text{B.29})$$

where $g_{a,h}$ ($a = 1-3$) are the holomorphic couplings for $U(1)_Y$, $SU(2)_L$, and $SU(3)_c$.

At $M_S < \mu < M_{\text{GUT}}$, the RG running of the holomorphic couplings is described by the MSSM beta functions at one-loop level as

$$\frac{dg_a}{d \log \mu} = \frac{1}{16\pi^2} b_a^{(1)} g_a^3, \quad b_a^{(1)} = \begin{pmatrix} 33/5 \\ 1 \\ -3 \end{pmatrix}. \quad (\text{B.30})$$

a runs over 1, 2, 3 for $U(1)_Y$, $SU(2)_L$, and $SU(3)_c$, respectively. By using RGEs in eq. (B.30), we evaluate the running of the holomorphic couplings for $SU(3)_c$, $SU(2)_L$, and $U(1)_Y$ given in eqs. (B.27)–(B.29). Then, we can obtain the GUT breaking VEV from $g_{a,h}(5\sqrt{2}\sigma) = g_{b,h}(5\sqrt{2}\sigma)$ as shown in eq. (B.7). Note that in this analysis, we are also agnostic about the threshold correction of the GUT scale particles.

B.2 The case of $M_{\text{PQ}} < M_{\text{GUT}}$

Next, we consider the case of $M_{\text{PQ}} < M_{\text{GUT}}$. The holomorphic gauge coupling at $\mu = M_S$ is calculated from eq. (B.1) with $\mu = M_S$. Again we canonically normalize the chiral multiplets at $\mu = M_{\text{GUT}}$, i.e., we take $Z(M_{\text{GUT}}) = 1$. Then, we can calculate $Z_i(M_S)$ for chiral multiplet i from eq. (B.8). In this case, the RG running of couplings changes at M_{PQ} . Then, we derive the wave function renormalization factor for each MSSM chiral multiplet by integrating each anomalous dimension given in eqs. (B.9)–(B.17) from M_S to M_{GUT} , and obtain

$$Z_{Q_{1,2}}(M_S) = \left[\frac{g_{1,c}(M_{\text{PQ}})}{g_{1,c}(M_S)} \right]^{-1/99} \left[\frac{g_{2,c}(M_{\text{PQ}})}{g_{2,c}(M_S)} \right]^{-3} \left[\frac{g_{3,c}(M_{\text{PQ}})}{g_{3,c}(M_S)} \right]^{16/9} \\ \times \left[\frac{\tilde{g}_{1,c}(M_{\text{GUT}})}{\tilde{g}_{1,c}(M_{\text{PQ}})} \right]^{-1/309} \left[\frac{\tilde{g}_{2,c}(M_{\text{GUT}})}{\tilde{g}_{2,c}(M_{\text{PQ}})} \right]^{-1/5} \left[\frac{\tilde{g}_{3,c}(M_{\text{GUT}})}{\tilde{g}_{3,c}(M_{\text{PQ}})} \right]^{-16/33}, \quad (\text{B.31})$$

$$Z_{Q_3}(M_S) = \left[\frac{y_t(M_{\text{GUT}})}{y_t(M_S)} \right]^{1/3} \left[\frac{g_{1,c}(M_{\text{PQ}})}{g_{1,c}(M_S)} \right]^{10/297} \left[\frac{g_{2,c}(M_{\text{PQ}})}{g_{2,c}(M_S)} \right]^{-2} \left[\frac{g_{3,c}(M_{\text{PQ}})}{g_{3,c}(M_S)} \right]^{32/27} \\ \times \left[\frac{\tilde{g}_{1,c}(M_{\text{GUT}})}{\tilde{g}_{1,c}(M_{\text{PQ}})} \right]^{10/927} \left[\frac{\tilde{g}_{2,c}(M_{\text{GUT}})}{\tilde{g}_{2,c}(M_{\text{PQ}})} \right]^{-2/15} \left[\frac{\tilde{g}_{3,c}(M_{\text{GUT}})}{\tilde{g}_{3,c}(M_{\text{PQ}})} \right]^{-32/99}, \quad (\text{B.32})$$

$$Z_{\bar{U}_{1,2}}(M_S) = \left[\frac{g_{1,c}(M_{\text{PQ}})}{g_{1,c}(M_S)} \right]^{-16/99} \left[\frac{g_{3,c}(M_{\text{PQ}})}{g_{3,c}(M_S)} \right]^{16/9} \\ \times \left[\frac{\tilde{g}_{1,c}(M_{\text{GUT}})}{\tilde{g}_{1,c}(M_{\text{PQ}})} \right]^{-16/309} \left[\frac{\tilde{g}_{3,c}(M_{\text{GUT}})}{\tilde{g}_{3,c}(M_{\text{PQ}})} \right]^{-16/33}, \quad (\text{B.33})$$

$$Z_{\bar{U}_3}(M_S) = \left[\frac{y_t(M_{\text{GUT}})}{y_t(M_S)} \right]^{2/3} \left[\frac{g_{1,c}(M_{\text{PQ}})}{g_{1,c}(M_S)} \right]^{-2/27} \left[\frac{g_{2,c}(M_{\text{PQ}})}{g_{2,c}(M_S)} \right]^2 \left[\frac{g_{3,c}(M_{\text{PQ}})}{g_{3,c}(M_S)} \right]^{16/27} \\ \times \left[\frac{\tilde{g}_{1,c}(M_{\text{GUT}})}{\tilde{g}_{1,c}(M_{\text{PQ}})} \right]^{-22/927} \left[\frac{\tilde{g}_{2,c}(M_{\text{GUT}})}{\tilde{g}_{2,c}(M_{\text{PQ}})} \right]^{2/15} \left[\frac{\tilde{g}_{3,c}(M_{\text{GUT}})}{\tilde{g}_{3,c}(M_{\text{PQ}})} \right]^{-16/99}, \quad (\text{B.34})$$

$$Z_{\bar{D}_i}(M_S) = \left[\frac{g_{1,c}(M_{\text{PQ}})}{g_{1,c}(M_S)} \right]^{-4/99} \left[\frac{g_{3,c}(M_{\text{PQ}})}{g_{3,c}(M_S)} \right]^{16/9} \left[\frac{\tilde{g}_{1,c}(M_{\text{GUT}})}{\tilde{g}_{1,c}(M_{\text{PQ}})} \right]^{-4/309} \left[\frac{\tilde{g}_{3,c}(M_{\text{GUT}})}{\tilde{g}_{3,c}(M_{\text{PQ}})} \right]^{-16/33}, \quad (\text{B.35})$$

$$Z_{L_i}(M_S) = \left[\frac{g_{1,c}(M_{\text{PQ}})}{g_{1,c}(M_S)} \right]^{-1/11} \left[\frac{g_{2,c}(M_{\text{PQ}})}{g_{2,c}(M_S)} \right]^{-3} \left[\frac{\tilde{g}_{1,c}(M_{\text{GUT}})}{\tilde{g}_{1,c}(M_{\text{PQ}})} \right]^{-3/103} \left[\frac{\tilde{g}_{2,c}(M_{\text{GUT}})}{\tilde{g}_{2,c}(M_{\text{PQ}})} \right]^{-1/5}, \quad (\text{B.36})$$

$$Z_{\bar{E}_i}(M_S) = \left[\frac{g_{1,c}(M_{\text{PQ}})}{g_{1,c}(M_S)} \right]^{-4/11} \left[\frac{\tilde{g}_{1,c}(M_{\text{GUT}})}{\tilde{g}_{1,c}(M_{\text{PQ}})} \right]^{-12/103}, \quad (\text{B.37})$$

$$Z_{H_u}(M_S) = \left[\frac{y_t(M_{\text{GUT}})}{y_t(M_S)} \right] \left[\frac{g_{1,c}(M_{\text{PQ}})}{g_{1,c}(M_S)} \right]^{4/99} \left[\frac{g_{3,c}(M_{\text{PQ}})}{g_{3,c}(M_S)} \right]^{-16/9} \\ \times \left[\frac{\tilde{g}_{1,c}(M_{\text{GUT}})}{\tilde{g}_{1,c}(M_{\text{PQ}})} \right]^{4/309} \left[\frac{\tilde{g}_{3,c}(M_{\text{GUT}})}{\tilde{g}_{3,c}(M_{\text{PQ}})} \right]^{16/33}, \quad (\text{B.38})$$

$$Z_{H_d}(M_S) = \left[\frac{g_{1,c}(M_{\text{PQ}})}{g_{1,c}(M_S)} \right]^{-1/11} \left[\frac{g_{2,c}(M_{\text{PQ}})}{g_{2,c}(M_S)} \right]^{-3} \left[\frac{\tilde{g}_{1,c}(M_{\text{GUT}})}{\tilde{g}_{1,c}(M_{\text{PQ}})} \right]^{-3/103} \left[\frac{\tilde{g}_{2,c}(M_{\text{GUT}})}{\tilde{g}_{2,c}(M_{\text{PQ}})} \right]^{-1/5}, \quad (\text{B.39})$$

where $g_{a,c}$ ($a = 1-3$) are the canonical gauge couplings for $U(1)_Y$, $SU(2)_L$, and $SU(3)_c$, and $\tilde{g}_{a,c}$ ($a = 1-3$) are the canonical gauge couplings for $U(1)_2$, $SU(2)_2$, and $SU(3)_2$, respectively. Then, $g_{1,h}(M_S)$, $g_{2,h}(M_S)$, and $g_{3,h}(M_S)$ can be evaluated by plugging Z 's in eqs. (B.31)–(B.39) into eq. (B.27), eq. (B.28), and eq. (B.29), respectively.

At $M_S < \mu < M_{PQ}$, the RG running of the holomorphic couplings is described by the MSSM beta functions at one-loop level given in eq. (B.30) as same as the case of $M_{PQ} < M_{GUT}$. At the PQ breaking scale M_{PQ} , the gauge symmetry is spontaneously broken by the VEV ϕ of \bar{F}_q and $\bar{F}_{\bar{q}}$ as

$$SU(3)_1 \times SU(3)_2 \rightarrow SU(3)_c, \quad (B.40)$$

$$SU(2)_1 \times SU(2)_2 \rightarrow SU(2)_L, \quad (B.41)$$

$$U(1)_1 \times U(1)_2 \rightarrow U(1)_Y. \quad (B.42)$$

Then, the tree level matching conditions for the holomorphic couplings are given as

$$\frac{1}{g_{3,h}^2(\phi)} = \frac{1}{\tilde{g}_{3,h}^2(\phi)} + \frac{1}{g_{14,h}^2(\phi)}, \quad (B.43)$$

$$\frac{1}{g_{2,h}^2(\phi)} = \frac{1}{\tilde{g}_{2,h}^2(\phi)} + \frac{1}{g_{14,h}^2(\phi)}, \quad (B.44)$$

$$\frac{1}{g_{1,h}^2(\phi)} = \frac{1}{\tilde{g}_{1,h}^2(\phi)} + \frac{1}{g_{14,h}^2(\phi)}, \quad (B.45)$$

where $\tilde{g}_{a,h}$ ($a = 1-3$) are the holomorphic couplings for $U(1)_2$, $SU(2)_2$, and $SU(3)_2$, and $g_{14,h}$ is the holomorphic coupling for $SU(14)_1$. The holomorphic coupling for $SU(14)_1$ at ϕ is calculated by

$$\frac{1}{g_{14,h}^2(\phi)} = \frac{b_{14}}{8\pi^2} \log \left(\frac{\phi}{\Lambda_{14}} \right), \quad (B.46)$$

where b_{14} is one-loop beta coefficient for $SU(14)_1$ and Λ_{14} is the dynamical scale of $SU(14)_1$.

At $M_{PQ} < \mu < M_{GUT}$, the RG running of the holomorphic couplings is described by the following one-loop beta functions;

$$\frac{dg_a}{d \log \mu} = \frac{1}{16\pi^2} b_a^{(1)} g_a^3, \quad b_a^{(1)} = \begin{pmatrix} 103/5 \\ 15 \\ 11 \\ -31 \end{pmatrix}. \quad (B.47)$$

a runs over 1, 2, 3, 14 for $U(1)_1$, $SU(2)_2$, $SU(3)_2$, and $SU(14)_1$, respectively. By using RGEs in eq. (B.47), we evaluate the running of the holomorphic couplings for $SU(3)_2$, $SU(2)_2$, and $U(1)_2$. Then, we can obtain the GUT breaking VEV from $\tilde{g}_{a,h}(5\sqrt{2}\sigma) = \tilde{g}_{b,h}(5\sqrt{2}\sigma)$ as shown in eq. (B.7). Note that in this analysis, we are also agnostic about the threshold correction of the PQ breaking and GUT scale particles.

	values
g_3	1.1525136966
g_2	0.64683244428
g'	0.35885152738
y_t	0.92377763013

Table 7. The list of input parameters

C RGEs

In this appendix, we summarize the values of the input parameters and the RGEs in the MSSM, the minimal SU(5) GUT, the MSSM with Georgi-Glashow type model, and the minimal SU(5) GUT with Georgi-Glashow type model. We show the two-loop beta functions for the gauge couplings and the one-loop beta functions for the top Yukawa coupling. We neglect other Yukawa couplings. The beta function coefficients are obtained from the generic formula given in Ref. [102].

C.1 Input parameters

Here we list the values of input parameters used for the analysis of RG running for gauge couplings and the top Yukawa coupling. We use the values of the input parameters for gauge couplings g' , g_2 , and g_3 and the top Yukawa coupling y_t at the renormalization scale $\mu = 200$ GeV in the $\overline{\text{MS}}$ scheme, which we take from Ref. [51]. Summarize these values in Tab. 7.

In our analysis, we use the $\overline{\text{DR}}$ scheme [103]. Then, we show the relations between the gauge couplings in the $\overline{\text{MS}}$ and $\overline{\text{DR}}$ scheme at one-loop level as follows [92, 104]:

$$g_a(\mu)_{\overline{\text{MS}}} = g_a(\mu)_{\overline{\text{DR}}} \left(1 - \frac{C(G_a)}{96\pi^2} g_a^2(\mu)_{\overline{\text{MS}}} \right). \quad (\text{C.1})$$

Here $C(G_a)$ is the quadratic Casimir invariant for the adjoint representations of group G_a . On the other hand, the relation between the Yukawa couplings in the $\overline{\text{MS}}$ and $\overline{\text{DR}}$ scheme at one-loop level is given as [104]:

$$(Y_k^{ij})_{\overline{\text{MS}}} = (Y_k^{ij})_{\overline{\text{DR}}} \left[1 + \sum_{a=1}^3 \frac{g_a^2}{32\pi^2} \{C(r_i) + C(r_j) - 2C(r_k)\} \right]. \quad (\text{C.2})$$

Here $C(r_i)$ is the quadratic Casimir invariant for the field with the subscript i .

C.2 MSSM

Here we discuss the MSSM whose matter content is given in Tab. 8. We introduce the top Yukawa coupling as $W = y_t Q_3 \bar{U}_3 H_u$. The two-loop RGEs for the gauge couplings are given as

$$\frac{dg_a}{d \log \mu} = \frac{1}{16\pi^2} b_a^{(1)} g_a^3 + \frac{g_a^3}{(16\pi^2)^2} \left[\sum_b b_{ab}^{(2)} g_b^2 - c_a y_t^2 \right]. \quad (\text{C.3})$$

	$U(1)_Y$	$SU(2)_L$	$SU(3)_c$
Q_i	1/6	\square	\square
\bar{U}_i	-2/3	1	$\bar{\square}$
\bar{D}_i	1/3	1	$\bar{\square}$
L_i	-1/2	\square	1
\bar{E}_i	1	1	1
H_u	1/2	\square	1
H_d	-1/2	\square	1

Table 8. The matter content in MSSM.

	$SU(5)_{\text{GUT}}$
Φ_i	$\bar{\square}$
Ψ_i	\square
H	\square
\bar{H}	$\bar{\square}$
Σ	adj

Table 9. The matter content in the minimal $SU(5)$ GUT.

a runs over 1, 2, 3 for $U(1)_Y$, $SU(2)_L$, and $SU(3)_c$, respectively. The beta function coefficients are given as

$$b_a^{(1)} = \begin{pmatrix} 33/5 \\ 1 \\ -3 \end{pmatrix}, \quad b_a^{(2)} = \begin{pmatrix} 199/25 & 27/5 & 88/5 \\ 9/5 & 25 & 24 \\ 11/5 & 9 & 14 \end{pmatrix}, \quad c_a = \begin{pmatrix} 26/5 \\ 6 \\ 4 \end{pmatrix}. \quad (\text{C.4})$$

The one-loop beta function of the top Yukawa coupling is given as

$$\frac{dy_t}{d \log \mu} = \frac{y_t}{16\pi^2} \left[6y_t^2 - \frac{13}{15}g_1^2 - 3g_2^2 - \frac{16}{3}g_3^2 \right]. \quad (\text{C.5})$$

See also Ref. [102] for details of beta functions in MSSM.

C.3 Minimal $SU(5)$ GUT

Here we discuss the minimal $SU(5)$ GUT whose matter content is given in Tab. 9. We introduce the top Yukawa coupling as $W = y_t \Psi_3 \Psi_3 H$. We do not include Σ^3 and $H \Sigma \bar{H}$ coupling in the superpotential. The two-loop beta function for the gauge coupling is given as

$$\frac{dg_5}{d \log \mu} = \frac{1}{16\pi^2} b^{(1)} g_5^3 + \frac{g_5^3}{(16\pi^2)^2} \left[b^{(2)} g_5^2 - c y_t^2 \right], \quad (\text{C.6})$$

where

$$b^{(1)} = -3, \quad b^{(2)} = 794/5, \quad c = 12. \quad (\text{C.7})$$

	U(1) _Y	SU(2) _L	SU(3) _c	SU(14) ₁
Q_i	1/6	\square	\square	1
\bar{U}_i	-2/3	1	$\bar{\square}$	1
\bar{D}_i	1/3	1	$\bar{\square}$	1
L_i	-1/2	\square	1	1
\bar{E}_i	1	1	1	1
H_u	1/2	\square	1	1
H_d	-1/2	\square	1	1
D_{14}	-1/3	1	\square	$\bar{\square}$
\bar{D}_{14}	1/3	1	$\bar{\square}$	$\bar{\square}$
L_{14}	-1/2	\square	1	$\bar{\square}$
\bar{L}_{14}	1/2	\square	1	$\bar{\square}$
A	0	1	1	\square

Table 10. The matter content in MSSM with Georgi-Glashow type model.

The one-loop beta function of the top Yukawa coupling is given as [57, 105]

$$\frac{dy_t}{d\log\mu} = \frac{y_t}{16\pi^2} \left[9y_t^2 - \frac{96}{5}g_5^2 \right]. \quad (\text{C.8})$$

C.4 MSSM with Georgi-Glashow type model

Here we discuss the MSSM with Georgi-Glashow type model whose matter content is given in Tab. 10. We introduce the top Yukawa coupling as $W = y_t Q_3 \bar{U}_3 H_u$. The two-loop beta functions for the gauge couplings are given as

$$\frac{dg_a}{d\log\mu} = \frac{1}{16\pi^2} b_a^{(1)} g_a^3 + \frac{g_a^3}{(16\pi^2)^2} \left[\sum_b b_{ab}^{(2)} g_b^2 - c_a y_t^2 \right], \quad (\text{C.9})$$

where

$$b_a^{(1)} = \begin{pmatrix} 103/5 \\ 15 \\ 11 \\ -31 \end{pmatrix}, \quad b_a^{(2)} = \begin{pmatrix} 1087/75 & 153/5 & 712/15 & 390 \\ 51/5 & 123 & 24 & 390 \\ 89/15 & 9 & 518/3 & 390 \\ 2 & 6 & 16 & -2941/7 \end{pmatrix}, \quad c_a = \begin{pmatrix} 26/5 \\ 6 \\ 4 \\ 0 \end{pmatrix}. \quad (\text{C.10})$$

The one-loop beta function of the top Yukawa coupling is given as

$$\frac{dy_t}{d\log\mu} = \frac{y_t}{16\pi^2} \left[6y_t^2 - \frac{13}{15}g_1^2 - 3g_2^2 - \frac{16}{3}g_3^2 \right]. \quad (\text{C.11})$$

C.5 Minimal SU(5) GUT with Georgi-Glashow type model

Here we discuss the minimal SU(5) GUT with Georgi-Glashow type model whose matter content is given in Tab. 11. We introduce the top Yukawa coupling as $W = y_t \Psi_3 \Psi_3 H$. We

	SU(5) ₂	SU(14) ₁
Φ_i	\square	1
Ψ_i	\square	1
H	\square	1
\bar{H}	\square	1
Σ	adj	1
\bar{F}_q	\square	\square
$\bar{\bar{F}}_{\bar{q}}$	\square	\square
A	1	\square

Table 11. The matter content in the minimal SU(5) GUT with Georgi-Glashow type model.

do not include Σ^3 and $H\Sigma\bar{H}$ coupling in the superpotential. The two-loop beta functions for the gauge couplings are given as

$$\frac{dg_a}{d\log\mu} = \frac{1}{16\pi^2} b_a^{(1)} g_a^3 + \frac{g_a^3}{(16\pi^2)^2} \left[\sum_b b_{ab}^{(2)} g_b^2 - c_a y_t^2 \right], \quad (\text{C.12})$$

where

$$b_a^{(1)} = \begin{pmatrix} 11 \\ -31 \end{pmatrix}, \quad b_a^{(2)} = \begin{pmatrix} 2166/5 & 390 \\ 48 & -2941/7 \end{pmatrix}, \quad c_a = \begin{pmatrix} 12 \\ 0 \end{pmatrix}. \quad (\text{C.13})$$

The one-loop beta function of the top Yukawa coupling is given as

$$\frac{dy_t}{d\log\mu} = \frac{y_t}{16\pi^2} \left[9y_t^2 - \frac{96}{5} g_5^2 \right]. \quad (\text{C.14})$$

D RGEs for proton decay

Here we briefly summarize the RGEs for proton decay operators. We only discuss the following dimension-six operators which are induced by the exchange of heavy gauge bosons:

$$\mathcal{L}_{\text{eff}} = C_{6(1)}^{ijkl} \epsilon_{abc} (u_{Ri}^a d_{Rj}^b) (q_{Lk}^c L_{Ll}) + C_{6(2)}^{ijkl} \epsilon_{abc} (q_{Li}^a q_{Lj}^b) (u_{Rk}^c e_{Rl}) + \text{h.c.} \quad (\text{D.1})$$

The RGEs for Wilson coefficients in the SM are given as [62]

$$\frac{d}{d\log\mu} C_{6(1)}^{ijkl} = \left(-\frac{11}{10} \frac{\alpha_1}{4\pi} - \frac{9}{2} \frac{\alpha_2}{4\pi} - 4 \frac{\alpha_3}{4\pi} \right) C_{6(1)}^{ijkl}, \quad (\text{D.2})$$

$$\frac{d}{d\log\mu} C_{6(2)}^{ijkl} = \left(-\frac{11}{10} \frac{\alpha_1}{4\pi} - \frac{9}{2} \frac{\alpha_2}{4\pi} - 4 \frac{\alpha_3}{4\pi} \right) C_{6(2)}^{ijkl}. \quad (\text{D.3})$$

Similarly, the RGEs in SUSY models (including MSSM) are [63]

$$\frac{d}{d\log\mu} C_{6(1)}^{ijkl} = \left(-\frac{11}{15} \frac{\alpha_1}{4\pi} - 3 \frac{\alpha_2}{4\pi} - \frac{8}{3} \frac{\alpha_3}{4\pi} \right) C_{6(1)}^{ijkl}, \quad (\text{D.4})$$

$$\frac{d}{d\log\mu} C_{6(2)}^{ijkl} = \left(-\frac{11}{15} \frac{\alpha_1}{4\pi} - 3 \frac{\alpha_2}{4\pi} - \frac{8}{3} \frac{\alpha_3}{4\pi} \right) C_{6(2)}^{ijkl}. \quad (\text{D.5})$$

Let us write the one-loop RGE for the gauge coupling as

$$\frac{dg_a}{d \log \mu} = \frac{1}{16\pi^2} b_a^{(1)} g_a^3, \quad (\text{D.6})$$

where a runs over 1, 2, 3 for $U(1)_Y$, $SU(2)_L$, and $SU(3)_c$, respectively. Then, the Wilson coefficients at the scale μ and μ_0 in the SM are related as

$$C_{6(1)}^{ijkl}(\mu) = \left(\frac{\alpha_1(\mu)}{\alpha_1(\mu_0)} \right)^{-11/20b_1^{(1)}} \left(\frac{\alpha_2(\mu)}{\alpha_2(\mu_0)} \right)^{-9/4b_2^{(2)}} \left(\frac{\alpha_3(\mu)}{\alpha_3(\mu_0)} \right)^{-2/b_3^{(2)}} C_{6(1)}^{ijkl}(\mu_0). \quad (\text{D.7})$$

Similar formula can be derived for $C_{6(2)}^{ijkl}$. Also, the Wilson coefficients at the scale μ and μ_0 in SUSY models are related as

$$C_{6(1)}^{ijkl}(\mu) = \left(\frac{\alpha_1(\mu)}{\alpha_1(\mu_0)} \right)^{-11/30b_1^{(1)}} \left(\frac{\alpha_2(\mu)}{\alpha_2(\mu_0)} \right)^{-3/2b_2^{(2)}} \left(\frac{\alpha_3(\mu)}{\alpha_3(\mu_0)} \right)^{-4/3b_3^{(2)}} C_{6(1)}^{ijkl}(\mu_0). \quad (\text{D.8})$$

Similar formula can be derived for $C_{6(2)}^{ijkl}$.

References

- [1] R. Jackiw and C. Rebbi, *Vacuum Periodicity in a Yang-Mills Quantum Theory*, *Phys. Rev. Lett.* **37** (1976) 172.
- [2] C. G. Callan, Jr., R. F. Dashen and D. J. Gross, *The Structure of the Gauge Theory Vacuum*, *Phys. Lett. B* **63** (1976) 334.
- [3] C. Abel et al., *Measurement of the Permanent Electric Dipole Moment of the Neutron*, *Phys. Rev. Lett.* **124** (2020) 081803 [[2001.11966](#)].
- [4] R. D. Peccei and H. R. Quinn, *CP Conservation in the Presence of Instantons*, *Phys. Rev. Lett.* **38** (1977) 1440.
- [5] R. D. Peccei and H. R. Quinn, *Constraints Imposed by CP Conservation in the Presence of Instantons*, *Phys. Rev. D* **16** (1977) 1791.
- [6] S. Weinberg, *A New Light Boson?*, *Phys. Rev. Lett.* **40** (1978) 223.
- [7] F. Wilczek, *Problem of Strong P and T Invariance in the Presence of Instantons*, *Phys. Rev. Lett.* **40** (1978) 279.
- [8] C. Vafa and E. Witten, *Parity Conservation in QCD*, *Phys. Rev. Lett.* **53** (1984) 535.
- [9] H. Georgi and L. Randall, *Flavor Conserving CP Violation in Invisible Axion Models*, *Nucl. Phys. B* **276** (1986) 241.
- [10] J. E. Kim, *A COMPOSITE INVISIBLE AXION*, *Phys. Rev. D* **31** (1985) 1733.
- [11] K. Choi and J. E. Kim, *DYNAMICAL AXION*, *Phys. Rev. D* **32** (1985) 1828.
- [12] L. Randall, *Composite axion models and Planck scale physics*, *Phys. Lett. B* **284** (1992) 77.
- [13] B. A. Dobrescu, *The Strong CP problem versus Planck scale physics*, *Phys. Rev. D* **55** (1997) 5826 [[hep-ph/9609221](#)].
- [14] M. Redi and R. Sato, *Composite Accidental Axions*, *JHEP* **05** (2016) 104 [[1602.05427](#)].

- [15] B. Lillard and T. M. P. Tait, *A Composite Axion from a Supersymmetric Product Group*, *JHEP* **11** (2017) 005 [[1707.04261](#)].
- [16] B. Lillard and T. M. P. Tait, *A High Quality Composite Axion*, *JHEP* **11** (2018) 199 [[1811.03089](#)].
- [17] H.-S. Lee and W. Yin, *Peccei-Quinn symmetry from a hidden gauge group structure*, *Phys. Rev. D* **99** (2019) 015041 [[1811.04039](#)].
- [18] M. B. Gavela, M. Ibe, P. Quilez and T. T. Yanagida, *Automatic Peccei-Quinn symmetry*, *Eur. Phys. J. C* **79** (2019) 542 [[1812.08174](#)].
- [19] L. Vecchi, *Axion quality straight from the GUT*, *Eur. Phys. J. C* **81** (2021) 938 [[2106.15224](#)].
- [20] R. Contino, A. Podo and F. Revello, *Chiral models of composite axions and accidental Peccei-Quinn symmetry*, *JHEP* **04** (2022) 180 [[2112.09635](#)].
- [21] P. Cox, T. Gherghetta and A. Paul, *A common origin for the QCD axion and sterile neutrinos from $SU(5)$ strong dynamics*, *JHEP* **12** (2023) 180 [[2310.08557](#)].
- [22] T. Gherghetta, H. Murayama and P. Quilez, *A High-Quality Composite Pati-Salam Axion*, [2505.08866](#).
- [23] C. Csáki, H. Murayama and O. Telem, *Some exact results in chiral gauge theories*, *Phys. Rev. D* **104** (2021) 065018 [[2104.10171](#)].
- [24] C. Csáki, H. Murayama and O. Telem, *More exact results on chiral gauge theories: The case of the symmetric tensor*, *Phys. Rev. D* **105** (2022) 045007 [[2105.03444](#)].
- [25] O. Aharony, J. Sonnenschein, M. E. Peskin and S. Yankielowicz, *Exotic nonsupersymmetric gauge dynamics from supersymmetric QCD*, *Phys. Rev. D* **52** (1995) 6157 [[hep-th/9507013](#)].
- [26] L. Alvarez-Gaume, J. Distler, C. Kounnas and M. Marino, *Softly broken $N=2$ QCD*, *Int. J. Mod. Phys. A* **11** (1996) 4745 [[hep-th/9604004](#)].
- [27] L. Alvarez-Gaume, M. Marino and F. Zamora, *Softly broken $N=2$ QCD with massive quark hypermultiplets. 2.*, *Int. J. Mod. Phys. A* **13** (1998) 1847 [[hep-th/9707017](#)].
- [28] S. P. Martin and J. D. Wells, *Chiral symmetry breaking and effective Lagrangians for softly broken supersymmetric QCD*, *Phys. Rev. D* **58** (1998) 115013 [[hep-th/9801157](#)].
- [29] H.-C. Cheng and Y. Shadmi, *Duality in the presence of supersymmetry breaking*, *Nucl. Phys. B* **531** (1998) 125 [[hep-th/9801146](#)].
- [30] M. J. Strassler, *Messages for QCD from the superworld*, *Prog. Theor. Phys. Suppl.* **131** (1998) 439 [[hep-lat/9803009](#)].
- [31] R. Kitano, *Hidden local symmetry and color confinement*, *JHEP* **11** (2011) 124 [[1109.6158](#)].
- [32] H. Murayama, *Some Exact Results in QCD-like Theories*, *Phys. Rev. Lett.* **126** (2021) 251601 [[2104.01179](#)].
- [33] E. Poppitz and S. P. Trivedi, *Some examples of chiral moduli spaces and dynamical supersymmetry breaking*, *Phys. Lett. B* **365** (1996) 125 [[hep-th/9507169](#)].
- [34] P. Pouliot, *Duality in SUSY $SU(N)$ with an antisymmetric tensor*, *Phys. Lett. B* **367** (1996) 151 [[hep-th/9510148](#)].

- [35] L. Randall and R. Sundrum, *Out of this world supersymmetry breaking*, *Nucl. Phys. B* **557** (1999) 79 [[hep-th/9810155](#)].
- [36] G. F. Giudice, M. A. Luty, H. Murayama and R. Rattazzi, *Gaugino mass without singlets*, *JHEP* **12** (1998) 027 [[hep-ph/9810442](#)].
- [37] A. Pomarol and R. Rattazzi, *Sparticle masses from the superconformal anomaly*, *JHEP* **05** (1999) 013 [[hep-ph/9903448](#)].
- [38] E. Farhi and L. Susskind, *Technicolor*, *Phys. Rept.* **74** (1981) 277.
- [39] G. Lazarides and Q. Shafi, *Axion Models with No Domain Wall Problem*, *Phys. Lett. B* **115** (1982) 21.
- [40] P. Pouliot and M. J. Strassler, *A Chiral $SU(n)$ gauge theory and its nonchiral $spin(8)$ dual*, *Phys. Lett. B* **370** (1996) 76 [[hep-th/9510228](#)].
- [41] M. A. Luty, *Naive dimensional analysis and supersymmetry*, *Phys. Rev. D* **57** (1998) 1531 [[hep-ph/9706235](#)].
- [42] A. G. Cohen, D. B. Kaplan and A. E. Nelson, *Counting 4 pis in strongly coupled supersymmetry*, *Phys. Lett. B* **412** (1997) 301 [[hep-ph/9706275](#)].
- [43] K. A. Intriligator and N. Seiberg, *Duality, monopoles, dyons, confinement and oblique confinement in supersymmetric $SO(N(c))$ gauge theories*, *Nucl. Phys. B* **444** (1995) 125 [[hep-th/9503179](#)].
- [44] J. D. Wells, *PeV-scale supersymmetry*, *Phys. Rev. D* **71** (2005) 015013 [[hep-ph/0411041](#)].
- [45] M. Ibe, T. Moroi and T. T. Yanagida, *Possible Signals of Wino LSP at the Large Hadron Collider*, *Phys. Lett. B* **644** (2007) 355 [[hep-ph/0610277](#)].
- [46] L. J. Hall and Y. Nomura, *Spread Supersymmetry*, *JHEP* **01** (2012) 082 [[1111.4519](#)].
- [47] M. Ibe and T. T. Yanagida, *The Lightest Higgs Boson Mass in Pure Gravity Mediation Model*, *Phys. Lett. B* **709** (2012) 374 [[1112.2462](#)].
- [48] M. Ibe, S. Matsumoto and T. T. Yanagida, *Pure Gravity Mediation with $m_{3/2} = 10\text{--}100$ TeV*, *Phys. Rev. D* **85** (2012) 095011 [[1202.2253](#)].
- [49] A. Arvanitaki, N. Craig, S. Dimopoulos and G. Villadoro, *Mini-Split*, *JHEP* **02** (2013) 126 [[1210.0555](#)].
- [50] N. Arkani-Hamed, A. Gupta, D. E. Kaplan, N. Weiner and T. Zorawski, *Simply Unnatural Supersymmetry*, [1212.6971](#).
- [51] Z. Alam and S. P. Martin, *Standard model at 200 GeV*, *Phys. Rev. D* **107** (2023) 013010 [[2211.08576](#)].
- [52] M. E. Machacek and M. T. Vaughn, *Two Loop Renormalization Group Equations in a General Quantum Field Theory. 1. Wave Function Renormalization*, *Nucl. Phys. B* **222** (1983) 83.
- [53] M. E. Machacek and M. T. Vaughn, *Two Loop Renormalization Group Equations in a General Quantum Field Theory. 2. Yukawa Couplings*, *Nucl. Phys. B* **236** (1984) 221.
- [54] J. Hisano, T. Kuwahara and N. Nagata, *Grand Unification in High-scale Supersymmetry*, *Phys. Lett. B* **723** (2013) 324 [[1304.0343](#)].
- [55] J. Hisano, D. Kobayashi, T. Kuwahara and N. Nagata, *Decoupling Can Revive Minimal Supersymmetric $SU(5)$* , *JHEP* **07** (2013) 038 [[1304.3651](#)].

- [56] J. Hisano, *Proton decay in SUSY GUTs*, *PTEP* **2022** (2022) 12B104 [[2202.01404](#)].
- [57] J. Hisano, H. Murayama and T. Yanagida, *Nucleon decay in the minimal supersymmetric $SU(5)$ grand unification*, *Nucl. Phys. B* **402** (1993) 46 [[hep-ph/9207279](#)].
- [58] J. Hisano, D. Kobayashi and N. Nagata, *Enhancement of Proton Decay Rates in Supersymmetric $SU(5)$ Grand Unified Models*, *Phys. Lett. B* **716** (2012) 406 [[1204.6274](#)].
- [59] J. L. Evans, N. Nagata and K. A. Olive, *A Minimal $SU(5)$ SuperGUT in Pure Gravity Mediation*, *Eur. Phys. J. C* **79** (2019) 490 [[1902.09084](#)].
- [60] J. R. Ellis, M. K. Gaillard and D. V. Nanopoulos, *On the Effective Lagrangian for Baryon Decay*, *Phys. Lett. B* **88** (1979) 320.
- [61] PARTICLE DATA GROUP collaboration, S. Navas et al., *Review of particle physics*, *Phys. Rev. D* **110** (2024) 030001.
- [62] L. F. Abbott and M. B. Wise, *The Effective Hamiltonian for Nucleon Decay*, *Phys. Rev. D* **22** (1980) 2208.
- [63] C. Munoz, *Enhancement Factors for Supersymmetric Proton Decay in $SU(5)$ and $SO(10)$ With Superfield Techniques*, *Phys. Lett. B* **177** (1986) 55.
- [64] T. Nihei and J. Arafune, *The Two loop long range effect on the proton decay effective Lagrangian*, *Prog. Theor. Phys.* **93** (1995) 665 [[hep-ph/9412325](#)].
- [65] Y. Aoki, T. Izubuchi, E. Shintani and A. Soni, *Improved lattice computation of proton decay matrix elements*, *Phys. Rev. D* **96** (2017) 014506 [[1705.01338](#)].
- [66] SUPER-KAMIOKANDE collaboration, A. Takenaka et al., *Search for proton decay via $p \rightarrow e^+ \pi^0$ and $p \rightarrow \mu^+ \pi^0$ with an enlarged fiducial volume in Super-Kamiokande I-IV*, *Phys. Rev. D* **102** (2020) 112011 [[2010.16098](#)].
- [67] HYPER-KAMIOKANDE collaboration, K. Abe et al., *Hyper-Kamiokande Design Report*, [1805.04163](#).
- [68] B. Holdom and M. E. Peskin, *Raising the Axion Mass*, *Nucl. Phys. B* **208** (1982) 397.
- [69] B. Holdom, *Strong QCD at High-energies and a Heavy Axion*, *Phys. Lett. B* **154** (1985) 316.
- [70] M. Dine and N. Seiberg, *String Theory and the Strong CP Problem*, *Nucl. Phys. B* **273** (1986) 109.
- [71] J. M. Flynn and L. Randall, *A Computation of the Small Instanton Contribution to the Axion Potential*, *Nucl. Phys. B* **293** (1987) 731.
- [72] K. Choi and H. D. Kim, *Small instanton contribution to the axion potential in supersymmetric models*, *Phys. Rev. D* **59** (1999) 072001 [[hep-ph/9809286](#)].
- [73] P. Agrawal and K. Howe, *Factoring the Strong CP Problem*, *JHEP* **12** (2018) 029 [[1710.04213](#)].
- [74] M. Kawasaki and K. Nakayama, *Axions: Theory and Cosmological Role*, *Ann. Rev. Nucl. Part. Sci.* **63** (2013) 69 [[1301.1123](#)].
- [75] M. Kawasaki, T. Moroi and T. Yanagida, *Can decaying particles raise the upper bound on the Peccei-Quinn scale?*, *Phys. Lett. B* **383** (1996) 313 [[hep-ph/9510461](#)].
- [76] T. Banks, M. Dine and M. Graesser, *Supersymmetry, axions and cosmology*, *Phys. Rev. D* **68** (2003) 075011 [[hep-ph/0210256](#)].

- [77] M. Kawasaki, T. T. Yanagida and N. Yokozaki, *Cosmological problems of the string axion alleviated by high scale SUSY of $m_{3/2} \simeq 10\text{--}100\text{TeV}$* , *Phys. Lett. B* **753** (2016) 389 [[1510.04171](#)].
- [78] K. Holland, M. Pepe and U. J. Wiese, *The Deconfinement phase transition of $Sp(2)$ and $Sp(3)$ Yang-Mills theories in $(2+1)$ -dimensions and $(3+1)$ -dimensions*, *Nucl. Phys. B* **694** (2004) 35 [[hep-lat/0312022](#)].
- [79] J. Braun, A. Eichhorn, H. Gies and J. M. Pawłowski, *On the Nature of the Phase Transition in $SU(N)$, $Sp(2)$ and $E(7)$ Yang-Mills theory*, *Eur. Phys. J. C* **70** (2010) 689 [[1007.2619](#)].
- [80] G. Cossu, M. D’Elia, A. Di Giacomo, G. Lacagnina and C. Pica, *Monopole condensation in two-flavor adjoint QCD*, *Phys. Rev. D* **77** (2008) 074506 [[0802.1795](#)].
- [81] M. Hindmarsh, S. J. Huber, K. Rummukainen and D. J. Weir, *Numerical simulations of acoustically generated gravitational waves at a first order phase transition*, *Phys. Rev. D* **92** (2015) 123009 [[1504.03291](#)].
- [82] C. Caprini et al., *Science with the space-based interferometer eLISA. II: Gravitational waves from cosmological phase transitions*, *JCAP* **1604** (2016) 001 [[1512.06239](#)].
- [83] C. Caprini et al., *Detecting gravitational waves from cosmological phase transitions with LISA: an update*, *JCAP* **03** (2020) 024 [[1910.13125](#)].
- [84] M. Reichert, F. Sannino, Z.-W. Wang and C. Zhang, *Dark confinement and chiral phase transitions: gravitational waves vs matter representations*, *JHEP* **01** (2022) 003 [[2109.11552](#)].
- [85] N. Aggarwal et al., *Challenges and opportunities of gravitational-wave searches at MHz to GHz frequencies*, *Living Rev. Rel.* **24** (2021) 4 [[2011.12414](#)].
- [86] S. Bolognesi, K. Konishi and A. Luzio, *Anomalies and phases of strongly coupled chiral gauge theories: Recent developments*, *Int. J. Mod. Phys. A* **37** (2022) 2230014 [[2110.02104](#)].
- [87] S. Raby, S. Dimopoulos and L. Susskind, *Tumbling Gauge Theories*, *Nucl. Phys. B* **169** (1980) 373.
- [88] S. Dimopoulos, S. Raby and L. Susskind, *Light Composite Fermions*, *Nucl. Phys. B* **173** (1980) 208.
- [89] T. Appelquist, Z.-y. Duan and F. Sannino, *Phases of chiral gauge theories*, *Phys. Rev. D* **61** (2000) 125009 [[hep-ph/0001043](#)].
- [90] T. Gherghetta, H. Murayama, B. Noether and P. Quir  ez, *A High-Quality Axion from Exact SUSY Chiral Dynamics*, .
- [91] I. Affleck, M. Dine and N. Seiberg, *Dynamical Supersymmetry Breaking in Supersymmetric QCD*, *Nucl. Phys. B* **241** (1984) 493.
- [92] I. Antoniadis, C. Kounnas and K. Tamvakis, *Simple Treatment of Threshold Effects*, *Phys. Lett. B* **119** (1982) 377.
- [93] M. Dine and Y. Shirman, *Some explorations in holomorphy*, *Phys. Rev. D* **50** (1994) 5389 [[hep-th/9405155](#)].
- [94] J. Terning, *TASI 2002 lectures: Nonperturbative supersymmetry*, in *Theoretical Advanced Study Institute in Elementary Particle Physics (TASI 2002): Particle Physics and Cosmology: The Quest for Physics Beyond the Standard Model(s)*, pp. 343–443, 6, 2003, [[hep-th/0306119](#)].

- [95] K. A. Intriligator and P. Pouliot, *Exact superpotentials, quantum vacua and duality in supersymmetric $SP(N(c))$ gauge theories*, *Phys. Lett. B* **353** (1995) 471 [[hep-th/9505006](#)].
- [96] D. Finnell and P. Pouliot, *Instanton calculations versus exact results in four-dimensional SUSY gauge theories*, *Nucl. Phys. B* **453** (1995) 225 [[hep-th/9503115](#)].
- [97] V. A. Novikov, M. A. Shifman, A. I. Vainshtein and V. I. Zakharov, *Exact Gell-Mann-Low Function of Supersymmetric Yang-Mills Theories from Instanton Calculus*, *Nucl. Phys. B* **229** (1983) 381.
- [98] V. A. Novikov, M. A. Shifman, A. I. Vainshtein and V. I. Zakharov, *Supersymmetric Instanton Calculus (Gauge Theories with Matter)*, *Nucl. Phys. B* **260** (1985) 157.
- [99] V. A. Novikov, M. A. Shifman, A. I. Vainshtein and V. I. Zakharov, *The beta function in supersymmetric gauge theories. Instantons versus traditional approach*, *Phys. Lett. B* **166** (1986) 329.
- [100] M. A. Shifman and A. I. Vainshtein, *Solution of the Anomaly Puzzle in SUSY Gauge Theories and the Wilson Operator Expansion*, *Nucl. Phys. B* **277** (1986) 456.
- [101] D. Korneev, D. Plotnikov, K. Stepanyantz and N. Tereshina, *The NSVZ relations for $\mathcal{N} = 1$ supersymmetric theories with multiple gauge couplings*, *JHEP* **10** (2021) 046 [[2108.05026](#)].
- [102] S. P. Martin and M. T. Vaughn, *Two loop renormalization group equations for soft supersymmetry breaking couplings*, *Phys. Rev. D* **50** (1994) 2282 [[hep-ph/9311340](#)].
- [103] W. Siegel, *Supersymmetric Dimensional Regularization via Dimensional Reduction*, *Phys. Lett. B* **84** (1979) 193.
- [104] S. P. Martin and M. T. Vaughn, *Regularization dependence of running couplings in softly broken supersymmetry*, *Phys. Lett. B* **318** (1993) 331 [[hep-ph/9308222](#)].
- [105] B. D. Wright, *Yukawa coupling thresholds: Application to the MSSM and the minimal supersymmetric $SU(5)$ GUT*, [hep-ph/9404217](#).